University of Massachusetts Dartmouth

Department of Chemistry and Biochemistry

Cloning and Characterization of Heme Transport Proteins on the Outer and the Inner Membranes of *Pseudomonas Aeruginosa*

A Thesis in

Chemistry

by

Hasan Ilhan

Submitted in Partial Fulfillment of the

Requirements for the Degree of

Master of Science

May 2011

ABSTRACT

Cloning and Characterization of Heme Transport Proteins on the Outer and the Inner Membranes of *Pseudomonas Aeruginosa*
by Hasan Ilhan

Iron is an essential element for the body and plays important roles in bacterial virulence. Pathogenic bacteria *Pseudomonas aeruginosa* has evolved sophisticated heme uptake systems to steal iron from environment. One of the heme uptake system contains an outer membrane heme receptor (PhuR), a periplasmic heme transport protein (PhuT), an inner membrane heme permease (PhuU) coupled with an ATPase (PhuV) and associated protein (PhuW), and a cytosolic heme-binding protein (PhuS).

In this study, PhuW genes was cloned, over-expressed in *E. coli* and purified as a 32 kDa His-tagged protein. Heme-staining assays show that the isolated PhuW binds heme in vitro. Fluorescence and UV studies suggest that apo-PhuW binds heme in a 1:1 stoichiometry ($K_d \sim 81$ nM) and the ferric heme is 5-coordinate with tyrosine as a possible axial ligand. CD spectroscopic studies show a well-ordered helix-rich structure for PhuW and little secondary structure changes upon heme binding to apo-PhuW. PhuW is reduced by dithionite but not by either DTT or ascorbate. Multiple sequence alignment and homology modeling reveals that Tyr166 is strictly conserved and likely to be the heme ligand in PhuW.

The PhuUV (heme permease and ATPase components on the inner membrane) have been cloned into pET101D vector, and expressed in *E. coli*. PhuV was purified by Ni-NTA

affinity chromatography as a 30 kDa protein. Heme-free (apo) PhuV binds heme at 1:1 ratio with affinity at the submicromolar level, as revealed by UV-vis and fluorescent titrations. Titrations with imidazole and reduction by dithionite suggest that histidine is the possible ligand for the ferric heme iron in PhuV.

In order to characterize the other components in the heme uptake system, PhuR (wild type and a few mutations $PhuR^{F343C}$ and $PhuR^{A527C}$) have been cloned into pET101D vectors, and expressed in *E. coli*. PhuR (and its variants) was purified by Ni-NTA affinity chromatography as a 70 kDa protien. In vitro studies indicate that PhuR binds free heme in the presence of 1% octyl-polyoxyethylene. In order to use Förster Resonance Energy Transfer (FRET) technique to probe heme binding and heme transport process, PhuR was successfully labeled with Alexa Fluor 488 (AF488) via specifically engineered cysteine sites ($PhuR^{F343C}$ and $PhuR^{A527C}$). The fluorescence intensity of the AF-donor is quenched when the protein binds to heme (the acceptor) and it is found that apo-$PhuR^{F343C}$ and apo-$PhuR^{A527C}$ bind heme in a 1:1 stoichiometry, with affinity at 69 and 108 nM, respectively. The biochemical characterizations of these novel membrane-bound heme transport proteins will contribute to a better understanding of the bacterial heme transport pathway.

Keywords: *Pseudomonas aeruginosa*, cloning, heme transport, membrane protein, site directed mutagenesis, spectroscopy.

ACKNOWLEDGEMENTS

First, I would like to thank my thesis advisor Dr. Maolin Guo for his guidance, support, and encouragement during my MS thesis studies. Special thanks as well to Dr. Yong Tong for his supervision and encouragement during the experimental work and preparation of the thesis. Particular thanks should be given to my thesis committee members, Dr. Timothy Su and Dr. Harvey J. Hou, for their critical reading and assistance.

I also want to extend my appreciation to my fellow group-mates, Yibin Wei, Ziya Aydin, Yi Zhang, and Zhiwei Liu for their kindness and enlightening discussions.

Last I would also like to thank my parents Hakki and Nebahat Ilhan, my brothers Kadir, Huseyin and my sister Arzu for their support.

Special thanks go to Turkish Government and Turkish Ministry of National Education for their financial support during my study in the USA.

TABLE OF CONTENTS

LIST OF FIGURES

LIST OF ABBREVIATIONS

ABC: ATP-binding Cassette

BLASTP: Basic Local Alignment Search Tool for Protein

CD: Circular Dichroism

DMSO: Dimethyl Sulfoxide

DTT: Dithiothreitol

EPR: Electronic Paramagnetic Resonance

ExPASy: Expert Protein Analysis System

Fbp. Ferric ion-binding Protein

GAS: Group A Streptococcus

HTP: Periplasmic Heme Transport Protein

K_d: Dissociation Constant

KPB: Potassium Phosphate Buffer

LMCT: Ligand to Metal Charge-Transfer

Ni-NTA: Nickel Nitrilotriacetic acid

NJ: Neighbor-Joining

PCR: Polymerase Chain Reaction

Phu: Periplasmic Heme Uptake

PhuR: Outer membrane heme receptor protein

PhuT: Periplasmic heme transport protein

PhuU: An inner membrane heme permease protein

PhuV: An ATPase component

PhuW: Periplasmic Heme Transporter from *P. aeruginosa*

PhuUVW: Inner membrane ATPase and permease proteins

PMSF: Phenylmethylsulfonyl Fluoride

PSIPRED: Protein Structure Prediction Server

SDS-PAGE: Sodium Dodecyl Sulphate Polyacrylamide Gel Electrophresis

UV: Ultra Violet

CHAPTER 1: BACTERIAL HEME BINDING PROTEINS

1.1. Introduction

1.1.1 The Importance of Iron, Heme and Bacteria for Biological Systems

Iron is an essential element to practically all organisms, including bacteria (1,2). At the cellular level, it is involved in crucial biological processes such as photosynthesis, nitrogen fixation, the trichloroacetic acid (TCA) cycle, methanogenesis, H_2 production, oxygen transport, gene regulation, and DNA biosynthesis (2,5). Iron mainly exists in two oxidation redox states either the oxidized state Fe^{3+} or the reduced state Fe^{2+}, in the body. These redox forms can be found in variable spin forms which are high and low to make them remarkable prosthetic resources and versatile when they are incorporated into proteins as a catalytic center or electron carrier in numerous cellular reactions (5,6). The incorporation of iron into proteins allows regulation of the local redox potential (ranging from -300 to +700mV), geometry and spin state of the iron atoms, such that they can fulfill their essential biological function (5,7).

Although iron is one of the most abundant elements on earth and such a useful element in various biological processes, it catalyzes the production of toxic hydroxyl radicals (OH^-) from hydrogen peroxide (H_2O_2) (the Fenton reaction) or the production of hydroxyl radicals (OH^-) from superoxide (O^-) (the Haber-Weiss reaction (Figure 1.1)) (8,9,10). Oxygen radicals and peroxides are highly harmful and damaging to lipids, proteins, and nucleic acid in the cell. These damages may induce aging and various diseases such as

stroke and cancer, and several neurological disorders such as Parkinson's disease, Alzheimer's disease and atherosclerosis (11,12).

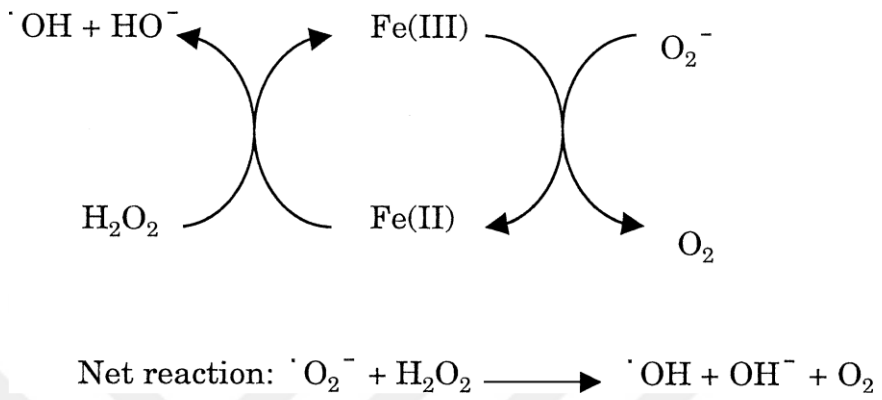

Figure 1.1: Fenton Reaction and Haber-Weiss Cycle. This scheme is commonly known as the Haber-Weiss cycle. Chemical reactions involve iron and the production of reactive oxygen species (13). The left-hand side of the cycle is the classical Fenton reaction (8,9).

Free iron is poorly available for bacteria inside animal hosts (free iron is at concentration below 10^{-18} M in human host (17). Upon access into a mammalian host, bacterial pathogens have adopted a set of control mechanisms to acquire and manage iron from tissues to survive. The first control is a high affinity transport system that efficiently scavenges iron in several forms from the host. Iron is commonly conserved within the cells in the form of protein-bound iron, which stores and control excess iron (14-15). Virtually all bacterial pathogens possess iron storage proteins to be infectious (16).

Three main mechanisms have been evolved by bacterial pathogens to accomplish the uptake of iron from the environment. A first common mechanism, bacterial pathogens

secrete and synthesize siderophores that actively chelate iron from the environment (18). The second mechanism, involved only in pathogenic bacteria, is to capture iron from the host iron binding proteins, such as transferrin, lactoferrin and ferritin via specific outer membrane receptors (9,15,18,19,20,21). The last method, also found mostly in bacterial pathogens, is to assimilate iron either from free heme or from hemoproteins, such as hemoglobin or hemopexin (22,23,24).

Heme is a prosthetic group that comprises of an iron atom and a protoporphyrin IX in many proteins such as hemoglobin and cytochromes (25). There are several types of hemes in biological molecules, for instance heme A, heme B and heme C. The biosynthetic precursor of each as a whole is heme B that is found in hemoglobin and carries propionyl groups in the porphyrin ring (26) (**Figure 1.2**). Heme is presented in the ferrous iron form (Fe^{2+}) that is highly reactive and thence useful cofactor in biological systems. Whereas the oxidized form (Fe^{3+}) is called hemin. Both the ferrous form and the ferric form are mostly known as "heme", which will be used throughout this thesis. Heme can also be used as a source of iron which plays a vital role in almost all organisms (26). Heme participates in electron transfer and respiration (cytochromes), oxygen storage and transport (myoglobin and hemoglobin), hydrogen peroxide degradation (peroxidases, catalases), oxygen sensing, activation of oxygen-containing molecules (P450 enzymes) (26,27), cellular signaling and gas sensing (28), apoptosis and regulation of DNA expression and enzymatic transformations of organic molecules (29). These properties are used in vivo to apply numerous biochemical and physiological roles. Heme

can also be a source of both iron and porphyrin for the microbes. Recently, by using ^{54}Fe-labeled heme and ^{57}Fe-labeled transferrin and analyzing the stable iron isotope contents of cells using inductively coupled plasma mass spectrometry (ICP-MS) which has been used to determine iron concentrations and isotope ratios in bacteria at many times during growth (2,30), Skaar and colleagues have revealed that the pathogenic bacterium *Staphylococcus aureus* prefers heme iron at its initial growth stage.

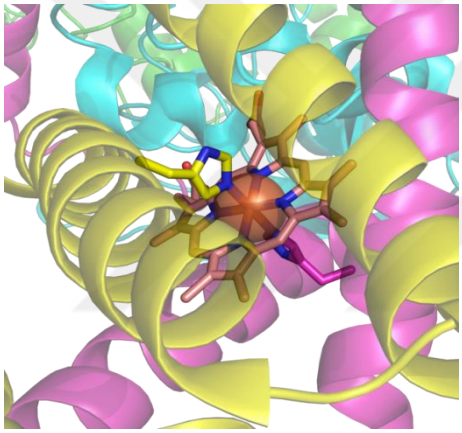

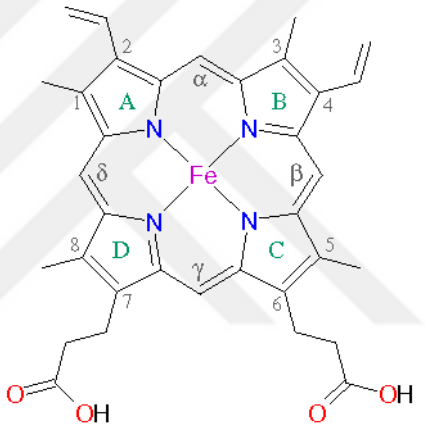

(A) **(B)**

Figure 1.2: The structure of Heme B. (A) The histidine bound heme group in a protein; (B) The structure of Heme B (31).

Heme B carries propionyl groups at positions 6 and 7 of the porphyrin ring according to Fisher system, and vinyl groups at location 2 and 4. Four methyl compounds occupy the remaining â-carbons and also have methyl groups at locations 1, 3, 5, and 8. The ferrous iron atom is coordinated by the nitrogen atoms at the center of the molecule (32,33).

Heme is poorly soluble in water at physiological pH but dissolves in the presence alkaline solution because of deprotonation of the propionic acid groups (34). It diffuses very slowly across membranes and has a tendency to form oxy-dimmers in the presence of oxygen. Heme is also a lipophilic molecule that can easily intercalate into cell membranes. Heme is a reactive molecule that promote the formation of reactive oxygen species (ROS). Accumulation of heme in cells may cause oxidative stress and tissue injury (35).

1.1.2 Iron Sources

The relatively insoluble ferric (Fe^{+3}) state is the major form of iron under conditions of aerobic and alkaline pH environments, but it is not directly assimilable by an organism. When in the Fe^{3+} state, iron will form large complexes with anions, water and peroxides. These large complexes have poor solubility and upon their aggregation lead to pathological consequences. Iron homeostasis requires the coordinated regulation of the synthesis and action of proteins involved in iron acquisition, utilization, and storage. When present in excess, iron is stored in a nontoxic form, in ferritins. Ferric iron (Fe^{3+}) is a widespread anaerobic terminal electron acceptor both for autotrophic and heterotrophic organisms. Electron flow in these organisms is similar to those in electron transport, ending in oxygen or nitrate. The ferrous (Fe^{+2}) state is favored at acidic pH and anaerobic conditions. The iron atom in the heme group must initially be in the ferrous (Fe^{2+}) oxidation state to support oxygen and other gases' binding and transport. This highly

soluble ion can transport through the outer membrane of gram negative bacteria strains and is transported through the cytoplasmic membrane (15,36) by a high affinity ferrous ion uptake (Feo) system that is essential for iron acquisition in many gram negative bacteria (15,37).

1.1.2.1 Transferrin and Lactoferrin

Most pathogenic bacteria can obtain iron from transferrin and lactoferrin as the typical iron sources (38). Transferrin is available in serum while lactoferrin is available in lymph and mucosal secretions (39). Transferrin functions as an iron transporter and as iron assimilation protein that contributes to the protection against microbial infections and iron toxicity, whereas lactoferrin has only protective function (40). Both proteins are monomeric glycoproteins with a molecular mass of about 80 kDa (15,41) and exhibit an extremely high affinity for the Fe^{3+} ion ($K_a \sim 10^{20}\ M^{-1}$) and a much lower affinity for Fe^{2+} ($10^3\ M^{-1}$).

1.1.2.2 Ferritins

Ferritin, consisting of 24 identical globular protein subunits filled with several thousands of Fe^{3+} ions, is the main iron storage in many organisms. These cytoplasmic proteins can be made available in case of an need of iron shortage, in which cells are protected from the toxic effects of free iron accumulation(15,39).

1.1.3 Heme Sources

Heme, a prosthetic group of hemoglobin, myoglobin and some enzymes, is composed of an iron atom in the center of a porphyrin ring. Due to its highly toxicity, it is scarcely found free, and therefore primarily bound to proteins like hemopexin or albumin (40). The heme containing proteins including hemoglobin, myoglobin, haptoglobin-hemoglobin complex, HAS, peroxidases, cytohchrome P450s and cytochromes, are present in bacteria, eukaryotic cells, and in the blood serum. Many bacterial pathogens have evolved several mechanisms for the scavenging of iron from host proteins. Hemoglobin and Myoglobin are very important oxygen transport proteins, and also the most abundant heme sources in the body (**Figure 1.3**) (41). However, like free heme, free hemoglobin is not tolerated by the body (42). Hemoglobin functions as the oxygen transporter, located in red blood cells. Each of the four subunits in hemoglobin binds a heme in which iron is penta-coordinated to four nitrogen atoms in the porphorin ring and one nitrogen on an imidazole ring of a histidine residue. The sixth coordination site binds to oxygen in oxyhemoglobin or to carbon dioxide in methemoglobin (the oxidized form of hemoglobin Fe^{3+}) (43). Hemoglobin dimers are bound with high affinity ($K_d \sim 10^{-12}$ M) by hemopexin or haptoglobin when heme is liberated through intravascular hemolysis during erythrocytes lysis (44). Then the haptoglobin-hemoglobin complex is subsequently recognized by CD163 receptor mediated endocytosis. The haptoglobin binds the hemoglobin which is released from erythrocytes by hemolysis. Myoglobin is a small, monomeric compact heme protein (MW ~ 17 800) which serves as an oxygen-binding protein pigment. It is found primarily in the skeletal muscle of vertebrates, and

functions in the storage of oxygen and is responsible for the transport of oxygen to the mitochondria for oxidative phosphorylation (45).

Hemopexin is a 60-kDa plasma glycoprotein with a high affinity to heme ($K_d \sim 10^{-13}$ M) in an equimolar ratio and delivers heme to the liver cells via receptor-mediated endocytosis (46,47). Hemopexin is an important heme transportation vehicle in the plasma and act as an extra cellular antioxidant, preventing heme-mediated oxidative stress. This protein involves two non-disulfide-linked domains, a 35-kDa N-terminal domain (domain I) that binds heme and a 25-kDa C-terminal domain (domain II) that are linked to a hinge region (48).

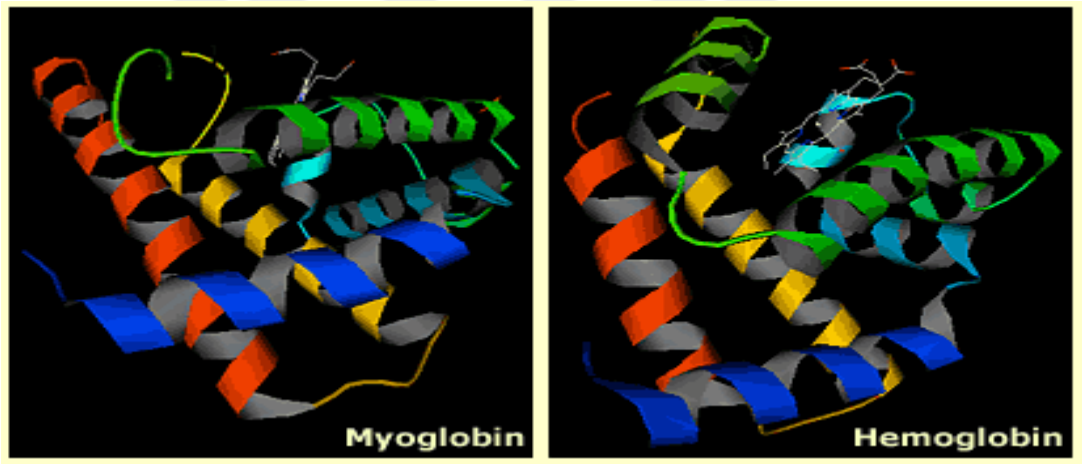

Figure 1.3: Structure of Myoglobin (A) and a subunit of hemoglobin (B) (41).

1.2. Overview of Bacterial Heme Uptake Systems

Many pathogenic bacteria can utilize heme to obtain iron needed for their survival (49-51). Heme is a required iron source of bacterial pathogens such as *Staphylococcus aureus* (2). Bacterial heme acquisition systems have been characterized in numerous bacterial

pathogens (52). The best known example of heme acquisition system is the uptake of heme through specific outer membrane receptors on the bacterial surface via direct binding of heme or heme proteins such as hemoglobin or hemopexin. The heme is then transported into the periplasm by ATP-binding cassette (ABC) transporters (51). Examples include the PhuRSTUVW system in *Pseudomonas aeruginosa* (51,53) and the ShuASTUV system in *Shigella dysenteria* (22,54). The second heme acquisition system is facilitated by the secretion of hemophores that bind heme and deliver it to specific outer receptors that interact with TonB-dependent (55,56) proteins. A common example of this strategy is the recently identified HasA/HasR system of *Serratia marcescens* (**Figure 1.4**) (15,57,58).

1.2.1 Hemophore-Mediated Heme Acquisition Systems

Hemophores are extracellular heme-binding proteins found only in gram-negative bacteria. Their function is to obtain free heme or extract heme and to deliver it to their specific outer membrane receptors (59). There are two species of the best characterized hemophore system so far. One hemophore system that has been characterized is heme acquisition system (HasA). The HasA is used by variable bacteria species, including pathogens in *Serratia marcescens* (51,57,58) and *Pseudomonas aeruginosa* (60,61). The second hemophore system that has been identified is heme/hemopexin utilization (HxuA) in *Hemophilus influenzae* (62,63). The *has* operon is under transcriptional control of the Fur (Ferric Uptake Regulator) repressor protein in conjunction with the specific

extracytoplasmic function ECF sigma and anti-sigma factors (**Figure 1.4**) (64,65). The *has* system has variable components that are utilized for heme uptake. HasA is a secreted hemophore that acquires heme outside the cell. HasA is proposed to remove the heme from its carrier, as opposed to forming a stable complex with hemoproteins (66). HasA is secreted from the cell by an ABC transporter complex that consists of three envelope proteins, HasD, HasE, and HasF (67). Has comprises the inner membrane portion of the secretory apparatus and is a part of the ABC proteins provided energy for the substrate export. HasE is also an inner membrane protein. HasF codes for the outer membrane portion of secretory complex (68). HasR is a specific outer membrane receptor of the HasA/heme complex. HasR can transport heme itself or regulate expression of the *has* operon with specific sigma and anti-sigma factors encoded by gene clustered at the *has* operon. HasB, a TonB homolog, provides the energy for movement of heme into the cell (69). The process by which heme is transported from the periplasmic space across the inner membrane has not been well described.

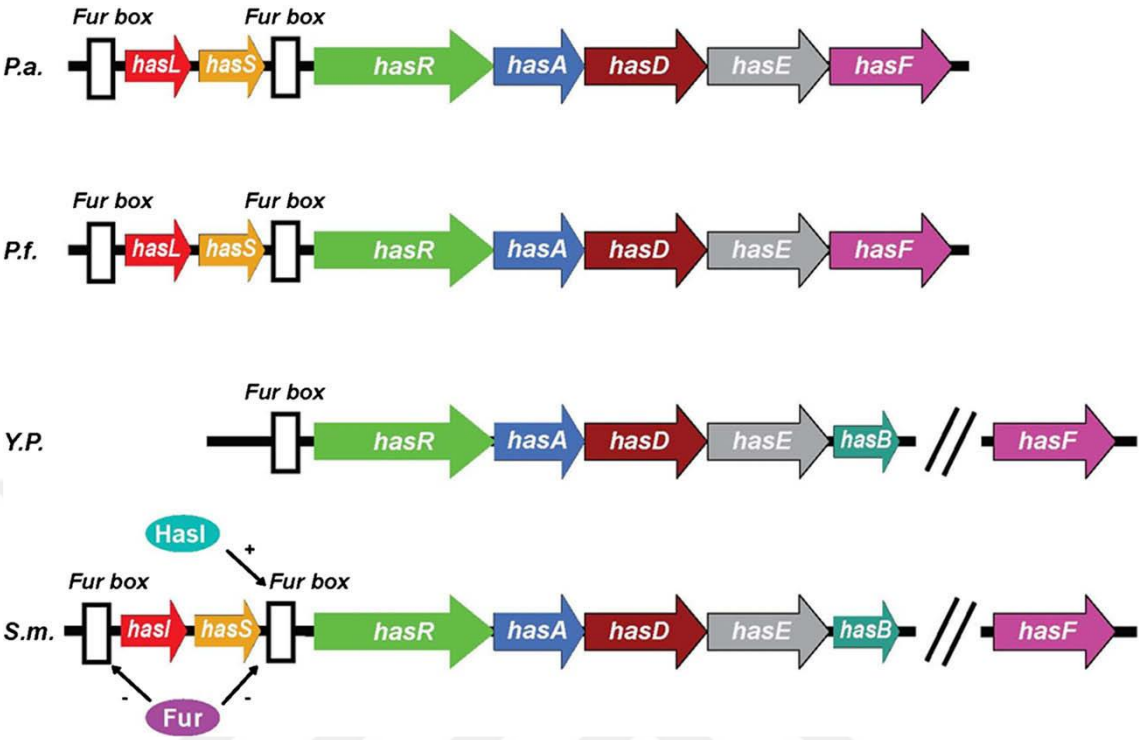

Figure 1.4: Genetic organization of the *has* systems in several bacteria. *P.a.*, *Pseudomonas aeruginosa*; *P.f., Pseudomonas fluorescens*; *Y.p., Yersinia pestis*; *S.m.*, *Serratia marcescens*. *HasI* and *hasS* encode sigma factors, respectively. The white box indicates a consensus *Fur* box (15,51).

.

The *hasA* hemophore from *S. marcescens* functions as a 19 kDa small polypeptide that removes heme from several heme containing proteins, and binds one b-type heme per molecule with high affinity (K_d lower than 10^{-8} M) (70). The crystal structure of heme-hasA complex has been characterized at 1.9 Å resolution showing that the heme iron is highly exposed to the solvent and is bound to residues His32 and Tyr75 (58,71). These may be significant to the function of hasA. HasA must interact with hemoglobin in such a way that it leads to a state in which its affinity for the heme ligand is greater than that of

the globin, and this will allow it to uptake to the periplasm *via* interaction with HasR, the TonB-dependent receptor (66).

The HxuA hemophore in *H. influenzae* is a 100 kDa extracellular protein that interacts with exogenous heme for aerobic growth. A gene cluster consisting of three genes, *hxuA*, *hxuB* and *hxuC*, is involved in the utilization of free heme and heme-hemopexin. All of them are necessary for effective growth on free heme and heme-hemopexin (63,72,73). HasA and HxuA hemophore proteins are commonly secreted into the extracellular medium, although their secretion systems are different: HasA is secreted by ABC transporters (HasDEF), but HxuA is secreted by a protein (HxuB) resembling transporters (60,61). The HxuC protein is a 78 kDa outer membrane protein and also is required for *H. influenzae* to acquire the low levels of heme (73).

1.2.2 Direct Heme Acquisition Systems in Gram Negative Bacteria

The direct heme uptake systems in gram-negative bacteria have been reported to play a significant role in *P. aeruginosa* infections (51). These systems also are similar and encoded by a ferric uptake regulator (*Fur*) gene cluster (**Figure 1.5**) and found in distinct loci in the genome (74). Two distinct heme uptake operons have been determined, including the *phu* (Pseudomonas heme utilization) and *has* (heme assimilation system) (75). The *phu* operon system contains PhuR which is a single outer membrane receptor (**Figure 1.7 A**)) and PhuSTUVW which encodes genes for a periplasmic binding protein

(PhuT) (**Figure 1.7 B**)), a cytoplasmic heme binding protein (PhuS), and inner membrane proteins (PhuUVW) (51) (**Figure 1.7** (**C**) **&** (**D**) and **Figure 1.6** the crystal structure of heme-bound ChaN) (76). A summary of the current understanding of a possible heme acquisition and transport in *P. aeruginosa* is presented in **Figure 1.8**. Once invaded into an animal host, bacterial pathogens produce hemolysin to lyse red blood cells in the form of hemoglobin and release hemoglobin (80-800 nM) into the serum. In the presence of the excess quantities of serum haptoglobin (5-20 µM), it combines rapidly with hemoglobin where it is delivered to the liver for removal. Hemopexin (12 µM, with a high affinity to heme K_d 10^{-13}) or Serum albumin (640 µM, K_d 10^{-18}) take up free heme released from hemoglobin or extract heme from hemoglobin. The bacteria heme outer membrane (OM) receptor (PhuR) can directly bind heme, hemoglobin, myoglobin, hemopexin, and haptoglobin-hemoglobin, assimilating the heme and transporting it via a TonB dependent process to the periplasmic (PP) heme transporter (PhuT) (51,77),

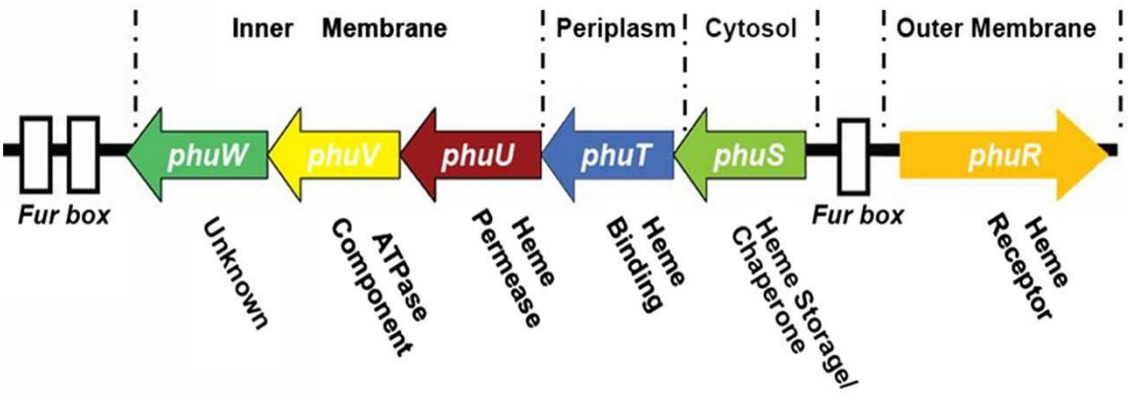

Figure 1.5: Map of the *P. aeruginosa* heme uptake locus containing the PhuR gene and the PhuSTUVW operon. Three Fur binding elements are indicated as white boxes.

which leads to shuttling of the heme between the outer and inner membrane (51). Heme is then translocated to the inner membrane (CM) by heme permease (PhuV), ATPase (PhuU) and an associated protein (PhuW). A cytoplasmic heme-binding protein (PhuS) stores the heme and delivers it to heme oxygenase (HO), which oxidizes heme and releases ferrous iron for bacterial growth (77,78).

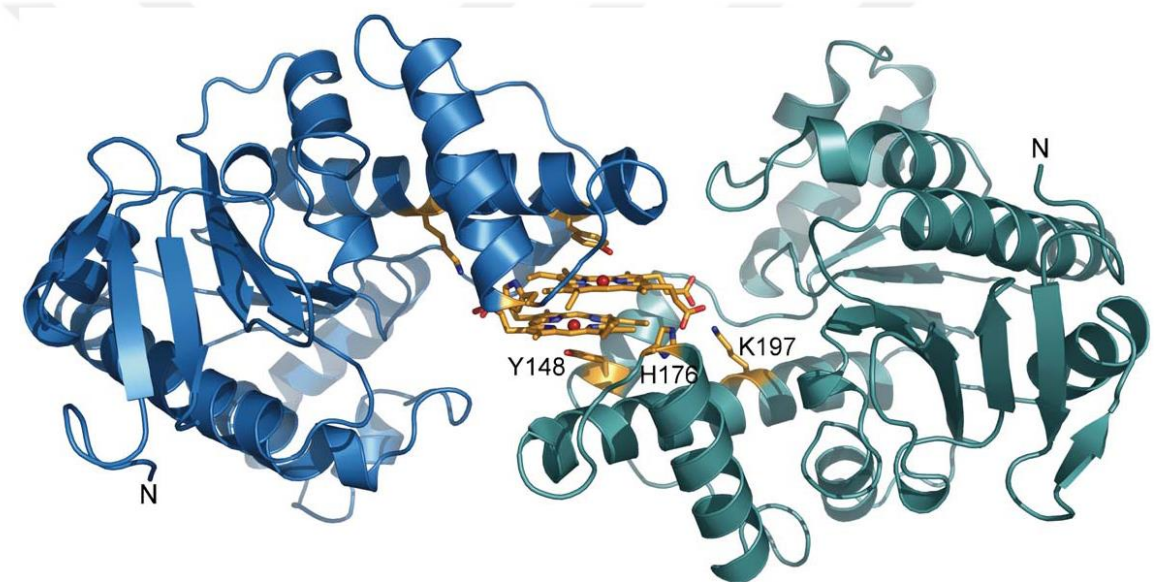

Figure 1.6: The crystal structure of heme-bound ChaN, a PhuW analogue in *Campylobacter jejuni*. Dimeric holo-ChaN encloses two cofacial heme molecules. ChaN is consisted of a large parallel β-sheet with flanking α-helices and a smaller domain consisting of α-helices. Two different colors, blue and teal, are used to show the two ChaN monomers. The heme and heme ligands are indicated as ball-and-stick representations and are colored in orange (76).

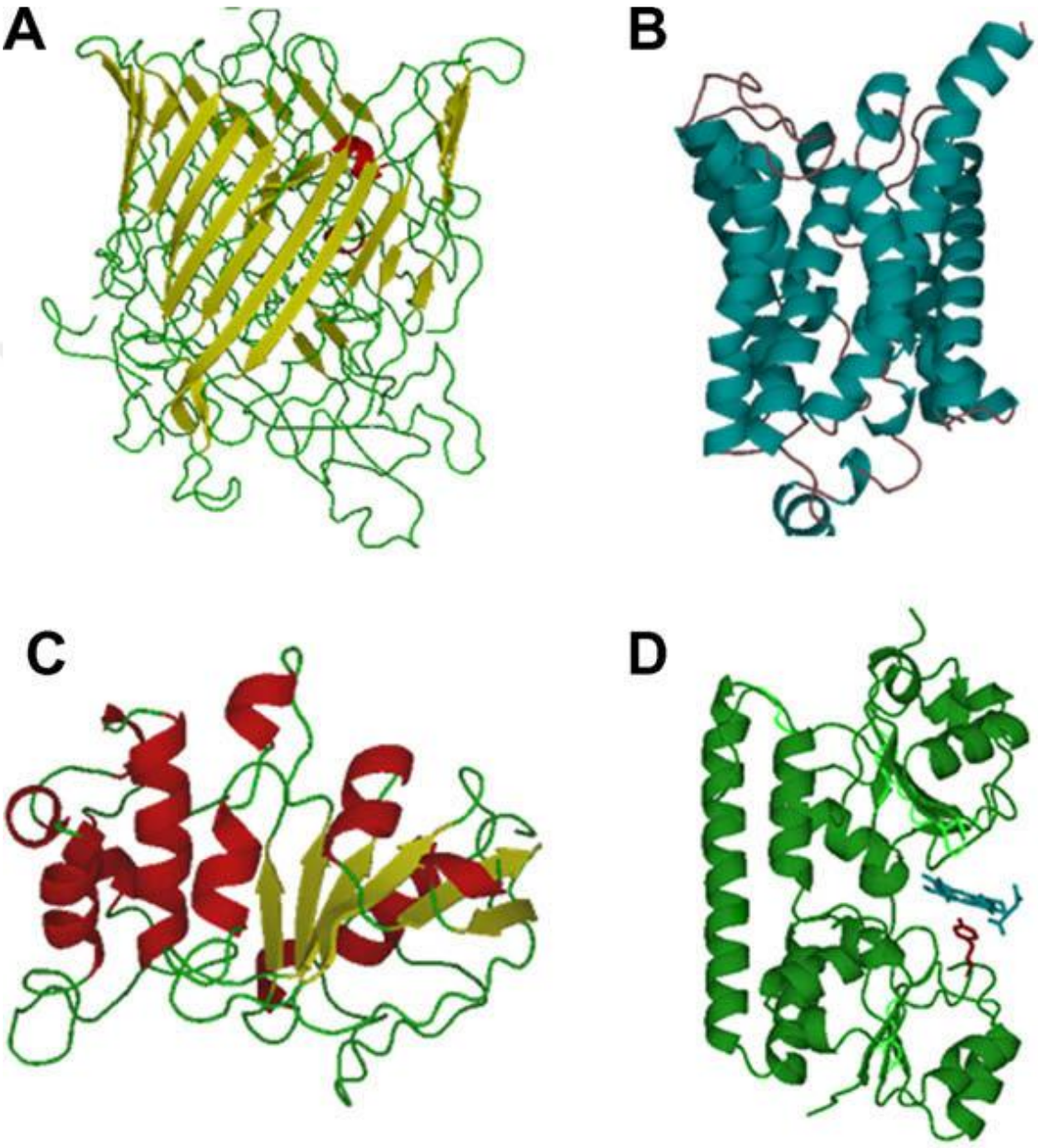

Figure 1.7: Homology models of heme transport proteins (PhuRUV) and crystal structure of heme transport protein (PhuT) of *P. aeruginosa* at the phu locus: (**A**) PhuR; (**B**) PhuT; (**C**) PhuU; (**D**) PhuV (51).

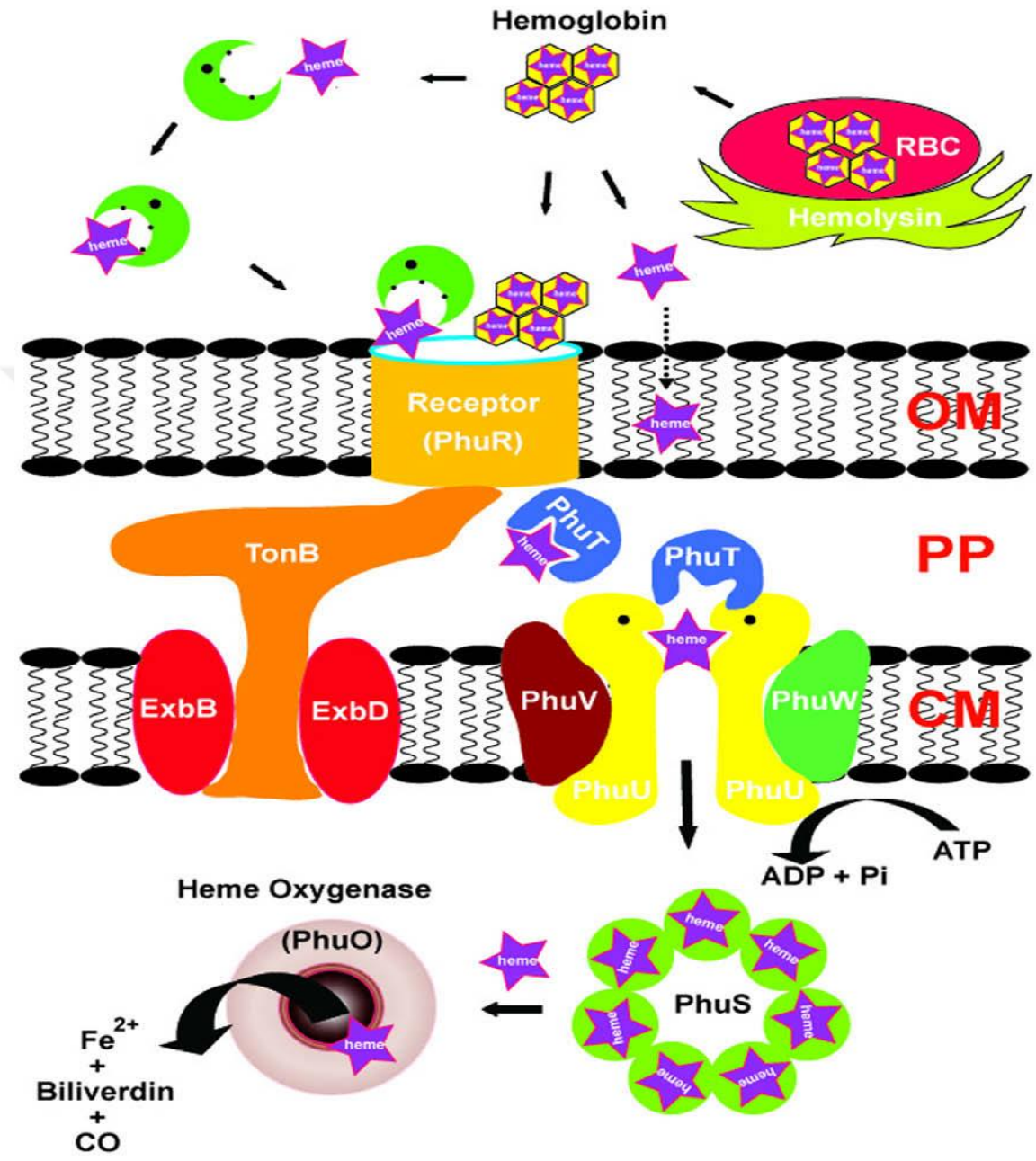

Figure 1.8: Heme Acquisition Systems in Gram Negative Bacteria *P. aeruginosa*.The proposed heme transport process in *P. aeruginosa*. Acquisition of iron is started by breaking red-blood cell by hemolysin (the green one). Albumin or hepexsin takes up free heme released from hemoglobin or extracts heme from hemoglobin and shuttles it to an

outer membrane receptor. Alternatively, receptor (PhuR) can directly bind heme/hemoglobin and transport heme across OM to PP by a TonB-dependent process. Periplasmic heme transport protein (PhuT) binds heme and transfers it to CM, then heme is translocated by heme permease (PhuU), ATPase (PhuV) and associated protein (PhuW). PhuS storages heme and delivers it to HO, which oxidizes heme and releases ferrous iron (51).

1.2.3 TonB-ExbB-ExbD System

Cytoplasmic membrane protein (CM) TonB provides energy for transport of heme into periplasmic space in many gram-negative bacteria. ExbB and ExbD are two cytoplasmic membrane proteins, which utilize the proton motive force to produce an energized form of TonB. The cellular ratio of TonB, ExbB and ExbD in *Escherichia coli* has been determined to be 1:7:2, respectively (79-81). The central proline-rich domain of TonB facilitates an extended rigid structure that allows TonB to span the periplasmic space (82). The CM TonB can be divided into three domains: a hydrophobic region at the N-terminal domain anchores the TonB protein to the CM and interacts with proteins ExbB and ExbD to form an energy transducing complex; the C-terminal domain of TonB directly contacts with the TonB-dependent receptors, particularly with their TonB box; and the intermediate domain involves a region of alternating Pro-Glu and Pro-Lys repeats in proline rich region. While ExbB contains three transmembrane segments in the cytoplasm, ExbD possesses only one transmembrane segment and most of the protein is available in the periplasm (83).

The three-dimensional crystal structure of two C terminal TonB were reported. One of the fragments is consisted of C terminal 85 amino acid residues of TonB and the other fragment is consisted of the C terminal 77 amino acid residues of TonB. Both fragments involve only residues 163-239 (84), because the eight additional N-terminal residues of TonB-85 are disordered, so it can not be determined in the electron density map. However, two fragments are significantly identical and indicate two molecules tightly engaged with each other as an intertwined dimmer (85).

Two systems for TonB-OM receptor interaction have been proposed (86). In the shuttle model, the energized form of TonB completely appears the CM, crosses the periplasmic space and transduces its energy to TonB dependent transporters (TBDTs) (87). In the pulling model, TonB remains membrane bound and spans the periplasmic space to interact with the TBDT. It is believed that conformational changes of TonB cause a pulling force on the plug domain of the TBDT that results in either a conformational change of the plug that remains in the barrel or a delocalization of the plug (88).

1.2.4 ABC Transport Systems

ABC transport systems (ATP-dependent transport systems) form a soluble periplasmic binding protein an integral inner membrane permease that is energized by a bound ATPase (5). They can mediate the import of heme, ferrous, ferric iron, and ferric irons coupled to siderophores and also are found for amino acids, peptides, sugars, and other

essential nutrients (22). Although these systems are substrate specific as identified by the ligand selection of periplasmic binding proteins and the permeases, they are used for the uptake of a wide variety of ligands. They are not interchangeable with each other in different systems (5,22,89).

1.2.4.1 Transport of Heme in the Periplasmic Space

Most of periplasmic binding proteins that have been structurally identified composed of two globular domains connected by short stretches of polypeptide chains which enable movement of the two lobes by a flexible hinge mechanism. Each lobe is comprised of a central β-sheet flanked by α-helices in the two globular domains (9,90). Due to the properties of the differences in domain structure and sequence of the periplasmic receptors, the structure of the binding site is efficiently variant (9).

After transport across the outer membrane, heme is inside periplasm space and then is sequestered by a heme-specific periplasmic binding protein (PhuT). Heme is transferred from PhuT to the cytoplasmic binding proteins (PhuUV) and ATPase (PhuW) through an ATP-binding cassette (ABC) transporter (51). To release iron from the heme molecule, the bacteria most likely employs a heme oxygenase (91).

Several periplasmic PhuTs have been described at genetic level, including HemT (*Y. enterocolitica*), ShuT (*Shigella dysenteriae*), PhuT (*P. aeruginosa*), HmuT (*C.*

diphtheriae), HutB (*Vibrio cholerae*), and ChuT (*E. coli*), that encode range from 30 to 90% identical amino acid residues (77).

The purpose of PhuTs is to bind heme in the periplasm and transfer it to the membrane-bound ABC transporter (92). It has been claimed that heme is present in a cleft between two subdomains of PhuT, that will lead to a conformational change in PhuT and this contributes to the holo form of PhuT to interact with the transmembrane domain of ABC transporter (51).

The best examples of identified periplasmic heme binding proteins are PhuT from *Pseudomonas aeruginosa* (51) and ShuT from *Shhigella dysenteria* (54). ShuT is a 28.5 kDa monomeric protein. The heme in ShuT is five-coordinated and high-spin with a Tyr proximal ligand. Wild type ShuT has a soret band at 400 nm and a few other bands 500, 521, and 617 nm (54). Further site directed mutagenesis studies indicated that Tyr-94 is the heme axial ligand. This was also confirmed by resonance Raman spectroscopy, magnetic circular dichroism spectroscopy and UV-visible spectroscopy. The structures of ShuT also indicated Tyr-94 on the heme binding pocket (54). PhuT is a 33 kDa heme binding protein with ~ 50% heme-bound in the native form. PhuT includes five-coordinate ferric heme center and the heme can be transferred to apo-myoglobin in vitro. PhuT is consisted of 24-26% α- helices, 20-21% of β-sheets, 19-22% of turns and 28-37% of other structures (56). PhuT showed a broad Soret band with maxima at 400 nm. The other weaker broad bands showed at 500, 534, and 624 nm. The heme in PhuT with addition of dithionite displayed a redshift of the 400, 500 and 534 nm bands to 420, 560

and 589 nm, respectively. A recent X-ray study has indicated that Tyr-71 is the axial ligand of PhuT. The heme binding pocket of PhuT also include charged residues, Arg73 and Arg228.

1.2.4.2 Transport of Heme Across the Cytosol

Once in the periplasm, heme is internalized by a periplasmic binding protein, which provides heme transfer to the cytoplasm through specific ABC transporters. The ABC transporters are comprised of periplasmic binding proteins, permeases, and ATPases, providing active translocation of various molecules across cell membranes via a lipid anchor in both gram-positive and gram-neagtive bacteria (22,93).

Several inner membrane proteins complete the transport of heme across the cytoplasmic membrane by utilizing an ABC transporter such as PhuU, PhuV and PhuW (51). Homology models of PhuU and PhuV were shown in **Figure 2.12**. Similar to that in ChaN, which is a putative lipoprotein from *Campylobacter jejuni*, PhuW shares 30% identical amino acid residues with ChaN and has been indicated to be essential in heme uptake in *P. aeruginoas* (77).

1.3 Heme Biosynthesis

Heme biosynthesis in eukaryotes occurs partly in the mitochondrion and partly in the cytosol, involving eight enzyme-catalyzed steps that serially convert glycine and

succinylCoA into heme (94). Most of the atoms in the heme molecule are derived from δ-aminolevulinic acid (ALA) or from an ALA precursor, for instance glutamic acid or succinic acid (94,95). An abbreviated scheme of the heme biosynthetic pathway can be seen in **Figure 1.9**.

The first step in heme biosynthesis starts in the mitochondrion with the condensation of 1 glycine and 1 succinylCoA by the pyridoxal phosphate containing enzyme ALA synthase to produce 5-aminolevulinic acid. This small molecule is the significant resource of all carbon and nitrogen atoms utilized for formation of tetrapyrrolic macrocycle (94-96),

Following synthesis, mitochondrial ALA is formed within the matrix of the mitochondrion and exported to the cytosol, where ALA dehydratese condenses 2 molecules of ALA to produce the pyrrole ring compound porphobilinogen (PBG). The third step in the pathway contains the head-to-tail condensation of four molecules of PBG to produce a linear tetrapyrrole intermediate, hydroxymethylbilane, a reaction catalyzed by PBG deaminase. Hydroxymethylbilane has two principal points. The most valuable point is conversion to uroporphyrinogen III, the next intermediate on the path to heme. This step is provided by uroporphrinogen synthase and uroporphyrinogen III cosynthase. This linear molecule cyclizes slowly (non-enzymatically) to generate uroporphyrinogen I (94-97).

In the cytosol, uroporphyrinogen decarboxylase enzyme catalyzes decarboxylation of all the acetate substituents of uroporphyrinogen III or uroporphyrinogen I to form coproporphyrinogen III. Coproporphyrinogen III is then transferred into the mitochondrion, where two of the propionate side chains and desaturation of porphyrin ring to vinyl groups leads to protoporphyrinogen IX, catalyzed by the enzyme coproporphyrinogen III oxidase. In the mitochondrion, the colorless product of protoporphyrinogen IX is a precursor for protoporphyrin IX which is created by the enzyme of protoporphyrin IX oxidase (94,95,99)

The last reaction in heme biosynthesis also occurs in the mitochondrion, contains the insertion of the ferrous form of iron into the ring system. Iron is transported in the plasma by transferrin, a protein that binds ferric ions. Ferrochelatase enzyme is converting protoporphyrin IX into heme in the eighth step of heme biosynthesis (94,99).

1.4. Heme Coordination

In the last few decades common studies of model hemes have been applied that are aimed at understanding the effect of axial ligands and porphyrin substituents on the electronic ground state and detailed magnetic properties of these systems themselves, as well as how they associated with the properties of heme uptake proteins (100). The common qualification of many of the heme uptake proteins in nearly examined studies is the ability to stabilize the heme in the ferric state (22).

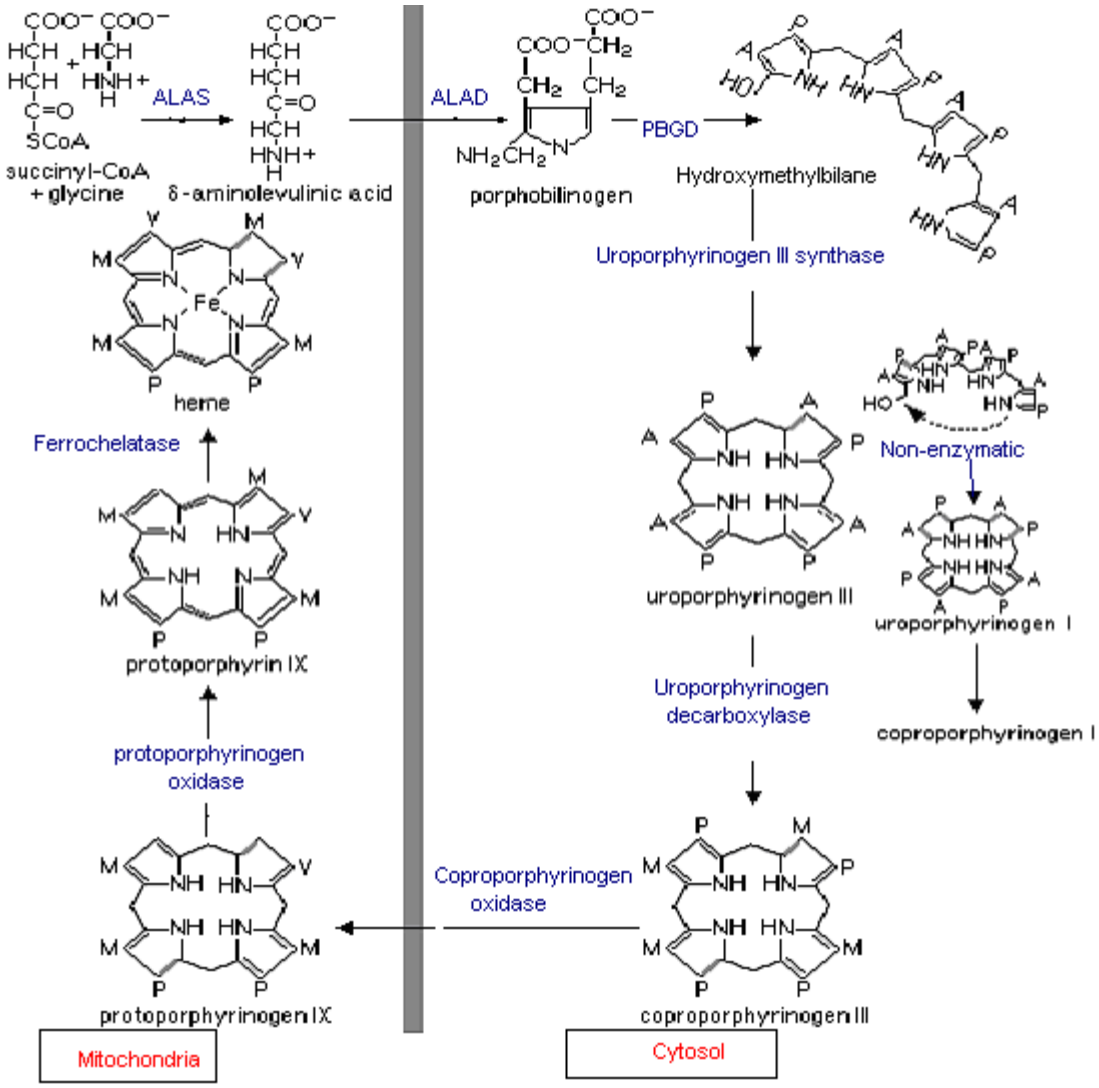

Figure 1.9: Pathway of Heme Biosynthesis. The first and the final three enzymes *δ*-aminolevulinic acid synthase (ALAS), Ferrochelate and protoporphrinogen oxidase are situated in the mitochondria and the remaining in the cytosol. The heme biosynthetic pathway involves four basic processes: formation of the pyrrole, assembly of the tetrapyrrole, modification of the tetrapyrrole side-chains followed by oxidation of protoporphyrinogen IX to protoporphyrin IX and insertion of a single ferrous iron to form heme. This final step, the insertion of iron into the protoporphyrin molecule, is catalyzed by the enzyme ferrochelatase. **Figure 1.9** is marked: ALAD = *δ*-aminolevulinic acid dehydratase, PBGD = porphobilinogen deaminese.

Furthermore, while heme contributes to mediate several responses, it is the interaction of heme with diverse coordinating proteins that eventually present molecular function. Structural insights facilitated from vibrational spectroscopy (EPR and Raman), nuclear magnetic resonance spectroscopy (NMR), and X-ray crystallography have showed that heme uptake proteins generally coordinate the iron center of the heme group between a histidine side chain and diverse other possible residues such as tyrosine (58), methionine (101), cysteine (102), proline (103), histidine (104), arginine (105).

The structure of sperm whale myoglobin is the first high resolution macro molecular structure identified by X-ray crystallography seating it within a hydrophobic pocket. It comprises of eight α-helices that wrap around the heme group (106). In the heme sequestering protein hemopexin found in serum, heme is coordinated between two -propeller domains (104), and in HasA the heme binding site is coordinated by a histidine (His-32) and a Tyr (Tyr-75) (**Figure 1.10**). This facilitates the first paradigm of a heme uptake protein with a Tyr ligand to the heme (71). A sole example of heme coordination in heme inner membrane proteins was recently reported for the heme regulated putative lipoprotein from *C. jejuni* ChaN, a PhuW analogue (**Figure 1.6**). ChaN function is poorly understood each heme iron is coordinated by a single tyrosine (Tyr-148) from one monomer, and the propionate groups are hydrogen bonded by a histidine and a lysine from the other monomer (76). The cytoplasmic heme binding protein, PhuS, has recently showed that it specifically transfers heme to the iron regulated heme oxygenase. The

heme is 6-coordinated through a His residue that is primarily low spin at neutral pH (107).

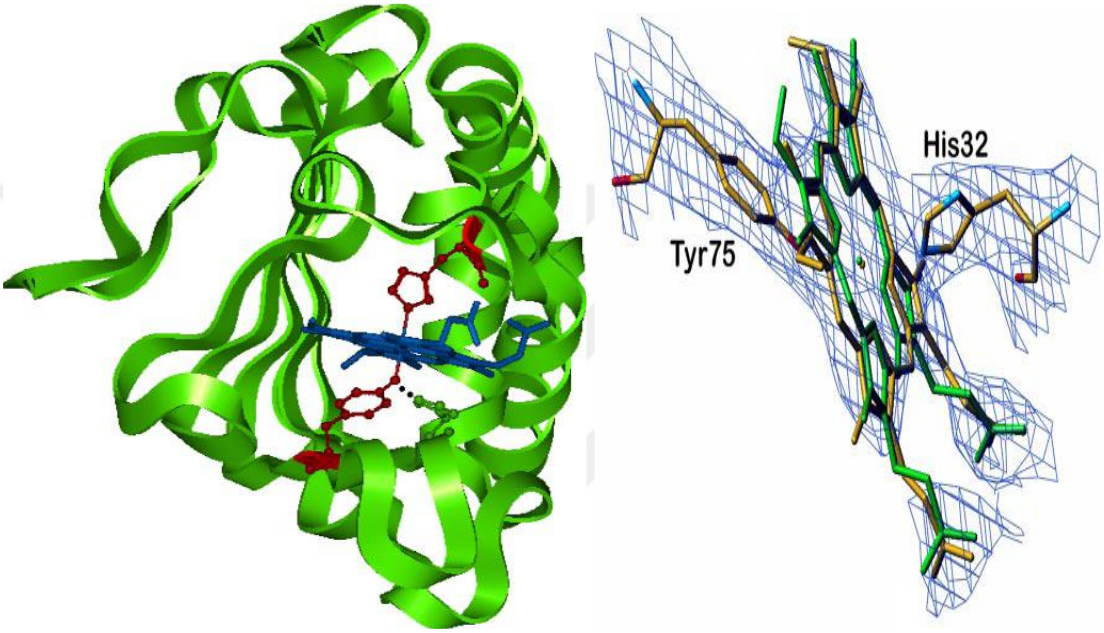

Figure 1.10: The structure of wild type holo-HasA (Protein Data Bank code 1B2V). The heme is in blue, and the two axial ligands, His32 and Tyr75, are in red. Residue His83, which is H-bonded to Tyr75, is in green on the left side. Right side shows final electron density of the heme region of H83A (Protein Data Bank code 2UYD).

1.5 Aims of This Thesis Work

The ability to transport heme is a significant virulence factor for bacterial pathogens. Most pathogenic bacteria require heme and have several sophisticated mechanisms to steal heme from the host. The understanding of heme transport pathways in bacteria has been advanced by the discovery of the bacterial heme transport gene clusters such as PhuRSTUVW in *P. aeruginosa*. The pariplasmic heme transport protein PhuT has been cloned and characterized by Guo's research group at UMASS Dartmouth (56) and the cytosol heme transport protein PhuS has been characterized by Wilks' lab (112). However, the membrane associated heme transport proteins, PhuR and PhuUVW, are still poorly understood. This work focuses on the cloning and characterization of the outermembrane heme receptor PhuR and innermembrane heme transport proteins PhuU, PhuV and PhuW. Mutations of the outer membrane protein PhuR and their roles in heme binding were also investigated.

1.6 References

1. Pohl, E., Haller, J. C., Mijovilovich, A., Meyer-Klaucke, W., Garman, E., and Vasil, M. L. (2003) Molecular Microbiology **47**, 903-915

2. Andreoni, F., Boiani, R., Serafini, G., Bianconi, I., Dominici, S., Gorini, F., and Magnani, M. (2009) Bioscience, Biotechnology, and Biochemistry **73**, 1180-1183

3. Rouault, T. A. (2004) Science **305**, 1577-1578

4. Poole, K., and Mckay, G. A. (2003) Bioscience **8**, 661-686

5. Crichton, R. Inorganic Biochemistry of Iron Metabolism, John Wiley and Sons, NY, 2001

6. Andrews, S. C., Robinson, A. K., and Rodriguez-Quinones, F. (2003) FEMS Microbiology Reviews **27**, 215-237

7. Liu, Z. D., and Hider, R. C. (2002) Coordination Chemistry Reviews **232**, 151-171

8. Ong, S. T., Ho, J. Z. S., Ho, B., and Ding, J. L. (2006) Immunobiology **211**, 295-314

9. Krieg, S., Huche, F., Diederichs, K., Puruneyra, N. I., Lecroisey, A., Wandersman, C., Delepelaire, P., and Welte, W. (2009) Proceedings of the National Academy of Sciences **106**, 1045-1050

10. Clarke, T. E., Tari, L. W., and Vogel, H. J. (2001) Medicinal Chemistry **1**, 7-30

11. Winterbourn, C. C. (1995) Toxicology Letters **82/83**, 969-974

12. Braun, V., and Killmann, H. (1999) Biochemistry Science **24**, 104-109

13. Arredondo, M., and Nunez, M. T. (2005) Molecular Aspects of Medicine **26**, 313-327

14. Pierre, J. L., and Fontecave, M. (1999) Biometals **12**, 195-199

15. Andrews, S. C., Smith, J. M. A., Yewdall, S. J., Guest, J. R., Harrison, P. M. (1991) FEBS Letters **293(1-2),** 164-168.

16. Wandersman, C., and Delepelaire, P. (2004) Annual Review of Microbiology **58**, 611-647

17. Skarr, E. P., and Schneewind, O. (2004) Microbes and Infection **6**, 390-397

18. Babakhanian, A., Gholivand, M.B., Mohammadi, A., Khodadadian, M., Shockravi,

A., Abbaszadeh, M., and Ghanbary, A. (2010) Journal of Hazardous Materials **177**, 159-166

19. Raymond, K. N., Dertz, E. A., and Kim, S. S. (2003) Proceedings of The National Academy of Sciences of U S A **100**, 3584-3588

20. Ratledge, C., and Dover, L. G. (2001) Annual Review of Microbiology **54**, 881-941

21. Guo, M., Harvey, I., Yang, W., Coghill, L., Campopiano, D. J., Parkinson, J. A., Macgillivray, R. T., Harris, W. R., and Sandler, P. J. (2003) Journal of Biological Chemistry **278**, 2490-2502

22. Butler, A. (2003) Natural Structural Biology **10**, 240-241

23. Wilks, A., and Burkhard, K. A. (2007) Natural Product Reports **24**, 511-522

24. Reniere, M. L., Torres, V. J., and Skaar, E. P. (2007) Biometals **20**, 333-345

25. Cescau, S., Cwerman, H., Letoffe, S., Delepelaire, P., Wandersman, C., and Biville, F. (2007) Biometals **20**, 603-613

26. Larsen, W. R., and Miksovka, J. (2007) Coordination Chemistry Reviews **251**, 1101-1127

27. Moraes, C. T., Diaz, C. T., and Barrientos A. (2004) Biochimica et Biophysica Acta**1659 (2-3)**, 153-159

28. Sudhamsu, J., Kabir, M., Airola, M. V., Patel B. A., Yeh, S. R., Rousseau, D. L., and Crane, B. R. (2010) Protein Expression and Purificitaion **73**, 78-82

29. Hamza, I., Chauan, S., Hassett, R., and O'Brian, M. R. (1998) The Journal Of Biological Chemistry **273**, 21669-21674

30. Hou, S., Reynolds, F., Horrigan, T. F., Heinemann, S. H., and Hoshi, T. (2006) American Chemical Society **39 (12)**, 918-924

31. Skaar, E. P., and Humayun, M. (2004) Science **305** (**5690**), 1626-1628

32. Huang, L., Sun, G., Cobessi, D., Wang, A.C., Shen, J.T., Tung, E.Y., Anderson, V.E., and Berry, E.A. (2006) Journal of Biological Chemistry **281**, 5965-5972

33. Iqbal, S. A., and Mido Y. Food Chemistry, Discovery Publishing House, India, 2005

34. Hansson, Mats., and Wachenfeldt, C. V. (1993) FEMS Microbiology Letters **107**, 121-125

35. Srivastava, A., and Beale, I. S. (2005) Journal of Bacteriology **187**, 4444-4450

36. Bach, F. H. (2005) The FASEB Journal **19**, 1216-1219

37. Gomez F. J. D., and Sansom, M. S. P. (2003) Nature Reviews Molecular Cell Biology **4**, 105-116

38. Mietzner, T. A., and Morse, S. A. (1994) Annual Review of Nutrition **14**, 471-493

39. Eichenbaum, Z., Muller, E., Morse, S. A., and Scott, J. R. (1996) Infection and Immunity **64**, 5428-5429

40. Finkelstein, R. A., Sciortino, C. V., and McIntosh, M. A. (1983) Reviews of Infectious Diseases **5**, 759-777

41. Torres, V. J., Pishchany, G., Humayun M., Schneewind, O., and Skaar, E. P. (2006) Journal of Bacteriology **188**, 8421-8429

42. Velayudhan, j., Hughes, N., Mccolm, A., Bagshaw, J., and Clayton, C. (2000) Molecular Microbiology **37**, 274-286

43. Scott D. G. O., and Schyvers, A. B. (1996) Trends in Microbiology 4, 185-191

44. Chasteen, N. D., and Harrison, P. M. (1999) Journal of Structural Biology **126**, 182-194

45. Dolphin, D., and Felton, F. H. (1974) Accounts of Chemical Research **7 (1),** 26-32

46. Ghigo, J. M., Letoffe, S., and Wandersman, C. (1997) The Journal of Bacteriology **179**, 3572-3579

47. Perutz, M. F., Rossman, M. G., Cullis, A. F., Muirhed, H., and North, A. C. T. (1960) Nature **185**, 416-422

48. Wejman, J. C., Hovsepian, D., Wall, J. S., Hainfeld, J. F., and Greer, J. (1984) Journal of Molecular Biology **174**, 319-341

49. Wittenberg, J. B., and Wittenberg, B. A. (1990) Annual Review of Biophysics and Biophysical Chemistry **19**, 217-241

50. Parkhurst, L. J. (1979) Annual Reviews of Physical Chemistry **30**, 503-546

51. Paoli, M., Anderson, B. F., Baker, H. M., Morgan, W. T., Smith, A., and Baker, E. N. (1999) Nature Structural Biology **6**, 926-931

52. Wu, M. L., and Morgan, W. T. (1995) Protein Science **4**, 29-34

53. Alam, J., and Smith, A. (1992) Journal of Biological Chemistry **267**, 16379-16384

54. Cavallaro, G., Decaria, L., and Rosato, A. (2008) Journal of Proteome Research **7**,

4946-4954

55. Krewulak, K.D., and Vogel, H. J., (2008) Biophysics Acta Biomembranes **1778**, 1781-1804

56. Tong, Y. and Guo, M. (2009) Archives of Biochemistry and Biophysics **481**, 1-15

57. Burkhard, K. A., and Wilks, A. (2008) Biochemistry **47**, 7977-7979

58. Ho, W. W., Li, H., Eakanunkul, S., Tong, Y., Wilks, A., Guo, M., and Poulos, T. L. (2007) Journal of Biological Chemistry **282**, 35796-35802

59. Eakanunkul, S., Lukat-Rodgers, G. S., Sumithran, S., Ghosh, A., Rodgers, K. R., Dawson, J. H., and Wilks, A. (2005) Biochemistry **44**, 13179-13191

60. Woloszczuk, W., Sprinson, D. B., and Ruis, H. (1980) Journal of Biological Chemistry **255**, 2624-2627

61. Zou, P., Borovok, I., Ortiz de Orue Lucana, D., Muller, D., and Schrempf, H. (1999) Microbiology **145** (**pt 3**), 549-559

62. Letoffe, S., Ghigo, J. M., and Wandersman, C. (1994) The Journal of Bacteriology **176**, 5372-5377

63. Arnoux, P., Haser, R., Izadi, N., Lecroisey, A., Delepierre, M., Wandersman, C., and Czjzek, M. (1999) Natural Structural Biology **6**, 516-520

64. Krieg, S., Huche, F., Diederichs, K., Izadi-Pruneyre, N., Lecroisey, A., Wandersman, C., Delepelaire, P., and Welte, W. (2009) Proceedings of The National Academy of Sciences of U S A **106**, 1045-1050

65. Letoffe, S., Omori, K., and Wandersman, C.(2000) The Journal of Bacteriology **182**, 4401-4405

66. Letoffe, S., Redeker, V., and Wandersman, C. (1998) Molecular Microbiology 28, 1223-1234

67. Hanson, M. S., Pelzel, S. E., Latimer, J., Muller-Eberhard, U., and Hansen, E. J. (1992) Proceedings of the National Academy of Sciences of USA **89**, 1973-1977

68. Cope, L. D., Thomas, S. E., Hrkal, Z., and Hansen, E. J. (1998) Infection and Immunity **66**, 4511-4516

69. Letoffe, S., Ghigo, J. M., and Wandersman, C. (1994). Proceedings of the National Academy of Sciences of USA **91**, 9876-9880

70. Rossi, M. S., Paquelin, A., Ghigo, J. M., and Wandersman, C. (2003) Molecular Microbiology **48**, 1467-1480

71. Letoffe, S., Nato, F., Goldberg, M. E., and Wandersman, C. (1999). Molecular Microbiology **33**, 546-555

72. Letoffe, S., Ghigo, J. M., and Wandersman, C. (1994). The Journal of Bacteriology **176**, 5372-5377.

73. Wandersman, C. (1998) Research in Microbiology **149**, 163-170

74. Paquelin, A., Ghigo, J. M., Bertin, S., and Wandersman, C. (2001) Molecular Microbiology **42**, 995-1005

75. Deniau, C., Gilli, R., Izadi-Pruneye, N., Letoffe, S., Delepierre, M., Wnadersman, C., Briand, C., and Lecroisey, A. (1997) Biochemistry **42**, 10627-10633

76. Caillet-Saguy, C., Turano, P., Piccioli, M., Lukat-Rodgers, G, S., Czjzek, M., and Guigliarelli, B. (2008) The Journal of Biological Chemistry **283**, 5960-5970

77. Cope, L. D., Thomas, S. E., Latimer, J. L., Slaughter, C. A., Muller-Eberhard, U., and Hansen, E. J. (1994) Molecular Microbiology **13**, 863-873

78. Cope, L. D., Yogev, R., Muller-Eberhard, U., and Hansen, E. J. (1995) The Journal of Bacteriology **177**, 2644-2653

79. Caillet-Saguy, C., Delepierre, M., Lecroisey, A., Bertini, I., Piccioli, M., and Turano, P. (2006) Journal of The American Chemical Society **128**, 150-158

80. Lansky, I. B., Lukat-Rodgers, G. S., Block, D., Rodgers, K. R., Ratliff, M., and Wilks, A. (2006) The Journal of Biological Chemistry **281**, 13652-13662

81. Chan, A. C. K., Lelj-Garolla, B. Rosell, F. I., Pedersen, K. A., Mauk, A. G., and Murphy, M. E. P. (2006) Journal of Molecular Biology **362**, 1108-1119

82. Stojiljkovic, I., and Perkins-Balding, D. (2002) DNA and Cell Biology **21**, 281-295

83. Friedman, J., Lad, L., Li, H., Wilks A., and Poulos, T.L. (2004) Biochemistry **43**, 5239-5245

84. Chang, C., Mooser, A., Plückthun, A., and Wlodawer, A. (2001) The journal of Biological Chemistry **276**, 27535-27540

85. Braun, V. (1995) The Federation of European Materials Societies Molecular Microbiology **24**, 271-283

86. Postle, K., and Skare, J. T. (1998) Journal of Biological Chemistry 263, 11000-11007

87. Postle, K. (1993) Journal of Bioenergetics and Biomembranes **25**, 591-601

88. Postle, K., and Kadner, R. J. (2003) Molecular Microbiology **49**, 869-882

89. Ködding, J., Killig, F., Polzer, P., Howard, S. P., Diederichs, K., and Welte, W. (2005) The Journal of Biological Chemistry **28**, 3022-3028

90. Pawelek, P. D., Croteau, N., Ng-Thow-Hing, C., Khursigara, C. M., Moiseeva, N., Allaire, M., and Coulton, J. W. (2006) Science **312**, 1309-1402

91. Mey, A. R., and Payne, S. M. (2002) The Journal of Bacteriology **185**, 1195-1207

92. Khursigara, C. M., Crescenzo, G. D., Pawelek, P.D., and Coultan, J. W. (2005) Protein Science **14**, 1266-1273

93. Schauer, K. Rodionov, D. A., and De Reuse, H. (2008) Trends in Biochemical Sciences **33**, 330-338

94. Sook, B. R., Block, D. R., Sumithran, S., Montanez, G. E., Rodgers, K. R., Dawson J. H., Eichenbaum, Z., and Dixon, D. W. (2008) Biochemistry **47**, 2678-2688

95. Braun, V., and Herrmann, C. (2007) The Journal of Bacteriology **189**, 6913-6918

96. Huber, W. J., and Backes, W. L. (2008) Analytical Biochemistry **373**, 167-169

97. Higgins, C. F., and Linton, K. J. (2004) Nature Structural & Molecular Biology 11, 918-926

98. Braun, V., and Götz, F. Microbial Fundamentals of Biotechnology, Wiley-WCH, Germany, 2007

99. Milgrom, L.R. The Colours of Life: An Introduction to the Chemistry of Porphyrins and Related Compounds, Oxford Press, Oxford, 1997

100. Heinemann, I. U., Jahn, M., and Jahn, D. (2008) Archives of Biochemistry and Biophysics **474**, 238-251

101. Ryter, S. W., and Tyrrell, R. M. (2000) Free Radical Biology & Medicine **28**, 289-309

102. O'Brian, M. R., (1996) Journal of Bacteriology **178**, 2471-2478

103. Voet, D., Voet, J. G., and Pratt, C. W. Fundamentals of Biochemistry, John Wiley & Sons, USA, 2009

104. De Matteis, F., and Marks, G. S. (1996) Journal of Physiology and Pharmacology

74(1), 1-8

105. Walker, F. A. (1999) Coordination Chemistry Reviews **185-186**, 471-534

106. Campos, A. P., Aguiar, A. P., Hervas, M., Regalla, M., Navarro, J. A., Ortega, J. M., Xavier, A. M., De La Rosa, M. A., and Teixeria, M. (1993) European Journal of Biochemistry **216**, 329-341

107. Dugad, L. B., Wang, X., Wang, C. C., Lukat, G. S., and Goff, H. M. (1992) Biochemistry **31**, 1651-1655

108. Lanzilotta, W. N., Schuller, D. J., Thorsteinsson, M. V., Kerby, R. L., Roberts, G. P., and Poulos, T. L. (2000) Natural Structural Biology **7**, 876-880

109. Paoli, M., Anderson, B. F., Baker, H. M., Morgan, W. T., Smith, A., and Baker, E. N. (1999) Natural Structural Biology **6**, 926-931

110. Suits, M. D., Jaffer, N., and Jia, Z. (2006) The Journal of Biological Chemistry **281**, 36776-36782

111. Kendrew, J.C. (1959) The Federation Proceedings **18**, 740-751

112. Kaur, A. P., Lansky, I. B., and Wilks, A. (2009) The Journal of Biological Chemistry **284**, 56-66

CHAPTER 2: CLONING AND EXPRESSİON OF A NOVEL INNER MEMBRANE HEME TRANSPORT PROTEIN FROM PSEUDOMONAS AERUGINOSA

2.1 Abstract

In this study an inner membrane heme transport protein from Pseudomonas aeruginosa, PhuW, was investigated. The *phuW* gene has been amplified by PCR (Polymerase Chain Reaction) and cloned into a pET101D vector. The positive clones were confirmed by DNA sequencing. The 32-kDa PhuW has been over expressed in *E. coli* and purified by Ni-NTA affinity column. The hemin binding properties of PhuW were studied by UV-vis, fluorescence, CD spectroscopies and heme staining. The data show that PhuW binds hemin in vitro at a 1:1 stoichiometry, with a broad Soret band at 409 nm and weaker β, α and CT bands at ~ 531 and 627 nm. Upon reduced, the soret band was sharpened and shifted to 412 nm, accompanied by red shifts of the β and α bands. Scatchard analysis gave a linear plot with a binding affinity (K_d) of 81 nM. CD spectroscopic studies reveal that PhuW is a helix-rich protein and heme binding induces little changes in its secondary structure. Multiple sequence alignment of the PhuW sequence to other putative inner membrane heme-binding proteins was performed to identify structurally conserved regions. A highly conserved tyrosine residue (Y166) is identified and it is most likely to be the heme ligand in PhuW, in agreement with the spectroscopic data. Structural modeling studies suggest that PhuW closely resembles the crystal structure of ChaN that shares 30% sequence identity with PhuW.

2.2. Introduction

Heme is a prosthetic group that comprises of iron and a protoporphyrin IX in many proteins such as hemoglobin and cytochromes. Heme can also be used as a source of iron which plays an essential role for bacterial growth of most bacteria in the host (1,2). However, due to low solubility of iron (III) at physiological pH in the presence of oxygen, iron uptake, transport, and storage is a critical obstacle for bacteria to overcome for survival and pathogenesis (3). The incorporation of iron into proteins as an electron transport or biocatalytic center facilitates organisms to carry out many crucial biological processes such as photosynthesis, N_2 fixation, methanogenesis, respiration, the tricarboxylic acid cycle, oxygen transport, control of gene expression, and DNA biosynthesis (4).

Pathogenic bacteria have developed sophisticated mechanisms to obtain iron from host. Most bacterial pathogens secrete and synthesize siderophores that actively chelate iron from their various sources (5). Alternatively, pathogens can also obtain iron directly from host sources such as heme, hemoglobin, or hemopexin via a specific outer membrane receptor that binds directly to host hemoproteins, extracting heme from the host (6).

Pseudomonase aeruginosa is known to be an opportunistic pathogen, producing a remarkable variety of virulence factors that is necessary for the infection of injured or immunocompromised hosts such as those with cancer or severe burns (7). *P. aeruginosa*

contains two heme uptake systems: Phu(Pseudomonas heme uptake) and Has (heme assimilation system) (8). The Phu system is comprised of an outer membrane receptor (PhuR), a periplasmic heme binding protein (PhuT), inner membrane ATPase and permease proteins (PhuUVW), and a cytoplasmic heme binding protein (PhuS) (1,9,10).

2.3 Experimental

2.3.1 Chemicals and Equipments

Restriction endonucleases were purchased from Fermentas (Canada). Hemin, sodium dithionite, sodium dodecyl sulfate, *o*-Dianisidine and sodium azide were obtained from Sigma. Protoporphyrin IX was purchased from TCI America. UV-vis spectra were measured on a Perkin-Elmer Lamda 25 spectrophotometer. Fluorescent spectra were measured on a Perkin-Elmer model LS55 luminometer. CD spectra were carried out using a Jasco J-715 spectropolarimeter (Jasco Corporation Tokyo, Japan).

2.3.2 Cloning of PhuW and Construction of Expression Vector

The gene encoding the inner membrane protein PhuW from *Pseudomonas aeruginosa* (12) was amplified from its genomic DNA (strain PAO1 from ATCC) via polymerase chain reaction (PCR). The following oligonucleotides (Qiagen Operon, FL): 5'-CACCATGCGCATTCGCCTGTTC-3' (T_m = 66 ˚ C) and 5'- ACGTGCC TTCT TCA TCTCCGCG-3' (T_m = 66 ˚ C) were used as the forward and reverse primers to amplify

PhuW gene with the stop codon truncated in order to be fused with a downstream His-tag sequence on the vector. The PCR products were then directly cloned into pET 101/D-TOPO vector (Invitrogen, CA) (See **Figure 2.1**) containing a built-in V5 epitope and a 6xHis tag sequence followed by a stop codon. The TOPO cloning products were then transformed into TOP10 One Shot™ competent *E. coli* cells (Invitrogen, CA), following the instructions in the manual and then plated on LB (Luria-Bertani) plate containing 100 μg/ml ampicilin at 37 ˚C overnight. Positive single colonies on the plate were inoculated in each of 5 ml small-scale culture in LB broth with shaking 220 rpm at 37 ˚C overnight. Plasmid DNA was isolated from these cultures using Qiagen's DNA Miniprep kits (Qiagen, CA) and screened by restriction enzymes Sac I/Xba I (Fermentas, Canada) double digestion followed by agarose gel electrophoresis. Positive plasmids containing the PhuW gene were confirmed by DNA sequencing at Cornell University (Cornell, NJ). The new construct is named pET101D/PhuW.

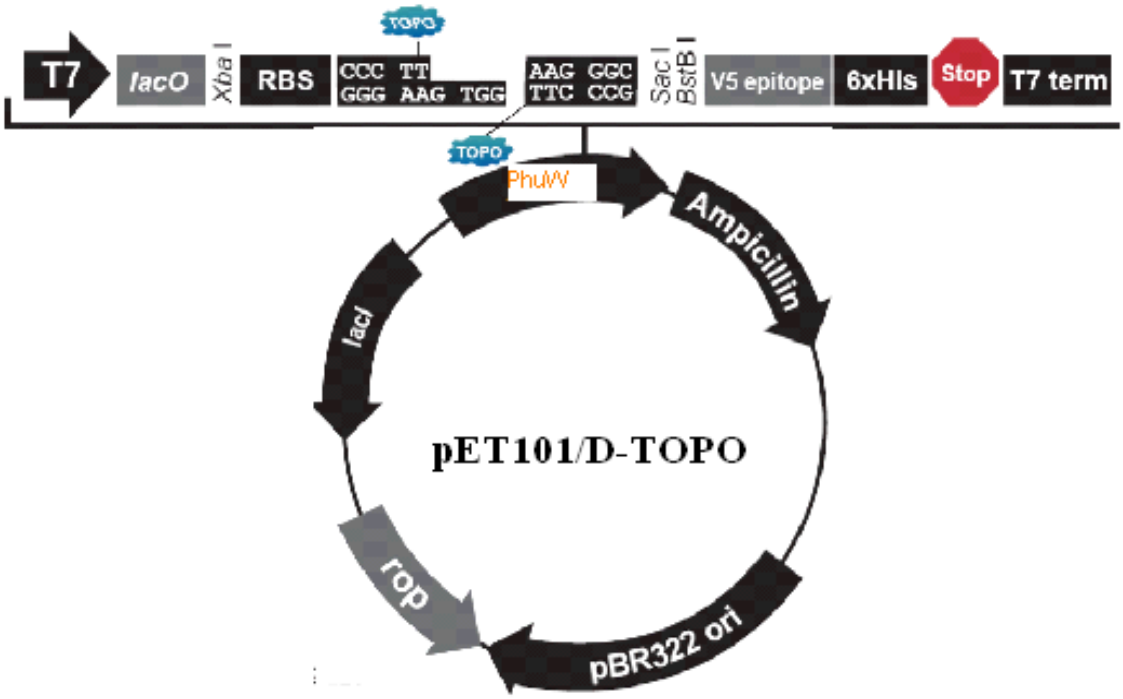

Figure 2.1: Map of the pET101/D-TOPO vector used in cloning of the PhuW gene.

2.3.3 Over-Expression and Purification of PhuW

BL21 (DE3) *E. coli* (Invitrogen, CA) cells were used for expressing the PhuW gene product. BL21 (DE3) *E. coli* cells were transformed with pET101D/PhuW, followed by plating on an LB plate with ampicilin (100 µg/ml). After overnight incubation at 37 ˚C, one single colony was picked up to inoculate each of 5 ml of LB broth containing 100 µg/ml ampicilin. These cultures were shaken at 220 rpm at 37 ˚C overnight and used to inoculate each 1 liter LB with 100 µg/ml ampicilin at 37 ˚C in 2.8 liter flasks. At OD_{600} ~ 0.8, 1 mM isopropyl beta-D-thiogalactoside (IPTG) was used for induction. The culture

was further shaken at 220 rpm, 37 ˚C overnight and harvested by centrifugation at 7000 rpm for 20 min. The pellets were collected and stored at -20 ˚C for protein purification.

Wild type recombinant PhuW was purified through Ni-NTA affinity column. The cell pellet was thawed at 4 ˚C for a while and re-suspended in 50 mM potassium phosphate buffer (KPB), pH 7.3, containing 300 mM NaCl, lysozyme (3g/liter), 1mM PMSF, 1 mM benzamidine, tiny amount of DNase and RNase, and then sonicated on ice for one min, alternating the power between on (0.5 second) and off (1.5 sec); this step was repeated 3 more times for a total of 3 min. Cell debris was removed by centrifugation. The supernatant was loaded onto a Ni-NTA affinity column (Qiagen, CA). The column was pre-equilibrated by 50 mM KPB containing 300 mM NaCl. Unbound proteins were removed by extensive washing with the buffer containing 5-10 mM imidazole. The PhuW protein was eluted by a step-wise procedure, using buffers containing 10, 20, 30 (?), 50, 100 and 500 mM imidazole. The fractions were collected and analyzed by SDS-PAGE. Most of the PhuW was found in the fractions containing 30 mM imidazole which was pooled with the first buffer wash and the initial flow through. The pure PhuW proteins were concentrated by ultra filtration using Amicon concentrator devices. PD-10 column was used to change KPB buffer and remove the excess of imidazole. Protein concentration was determined by the Bradford method (13) using bovine serum albmin as a standard, and then ε_{280} nm was determined by measuring the absorbance at 280 nm.

2.3.4 Heme Staining Assay

In order to detect whether the purified recombinant PhuW (wide type) involves heme or can bind heme in vitro, heme-specific staining procedure was applied for native PhuW and its mixture with hemin after separating the protein from unbound hemin by native PolyAcrylamide Gel Electrophoresis (PAGE). Gels and buffers were prepared according to the Laemmli method (14). Laemmli gels were equilibrated at 4 ˚C prior to electrophoresis. The buffer tank kept cooled with an ice bath during electrophoresis. Two identical wild type PhuW and four similar PhuW samples pre-loaded with hemin were loaded on the native gel at alternative positions. The electrophoresis was carried out between 4 mA to 7 mA (after the initial start at 70 V) for ~ 10 h. After the electrophoresis, the gel was divided into two pieces each containing a wild type PhuW sample and two samples with addition of heme. One gel piece was stained for protein peptides with Coomassie Blue and the second piece was stained for heme with *o*-Dianisidine dihydrochloride/H_2O_2 following a published procedure (15) with slight modification. The first gel involving Coomassie Blue gel was rinsed for 20 min in destain solution containing methanol/acetic acid/water = 3:1:6 (v/v/v), respectively. The second gel involving with *o*-Dianisidine dihydrochloride/H_2O_2 was washed for 15 min in methanol/sodium acetate (0.25 M, pH 5.0) = 3:7 (v/v), subsequently incubated in the dark for 30 min in a freshly prepared solution of 7 volume of 0.25 M sodium acetate, pH 5.0, and 3 volume of 6mM with *o*-Dianisidine dihydrochloride in methanol. Gels were developed for 60 min by adding H_2O_2 to a final concentration of 60 mM, washed for 20 min in H_2O/methanol/acetic acid = 8:1:1 (v/v/v), dried, and photographed.

2.3.5 Reduction of PhuW

Reduction of PhuW was measured by UV-vis spectroscopy in 20 mM potassium phosphate buffer (KPB), 100 mM NaCl, pH 7.4, on a Perkin-Elmer (Lamda 25) spectrophotometer. The reduced form of PhuW (1-10 μM) was obtained by addition of excess sodium dithionite (2-20 mM). Ascorbic acid (8-16 mM) and dithiothreitol (DTT, 1.7-15 mM) were also used to attempt to reduce PhuW.

2.3.6 Reconstitution with Heme or Protoporphyrin IX

In order to investigate if the apo-PhuW protein can bind heme or if it can bind Fe-free protoporphyrin IX, titration experiments were applied in 50 mM KPB, 300 mM NaCl (pH 7.2) and measured by UV-vis spectroscopy. Absorbance increase at 413 nm was measured for each addition of heme solution. Heme solution was freshly prepared in 0.1 M NaOH and concentrations were determined using $_{385}$ value of 58,440 $M^{-1}cm^{-1}$(16). Protoporphyrin IX was prepared as described previously (concentration was determined by using $_{406}$ = 242,000 $M^{-1}cm^{-1}$) (17).

2.3.7 Circular Dichroism (CD) Spectroscopy

Spectroscopic characterization of proteins is important for obtaining complete structural information. CD spectroscopy resembles UV-vis spectroscopy but involves a phase-

sensitive-detector (PSD). PSD is a special detector which extracts a small periodic signal of known frequency and phase from a large background of incoherent noise. Far UV CD (190-250 nm) studies were performed to obtain secondary structural information of apo- and holo-PhuW. This experiment was monitored on a Jasco J-715 spectropolarimeter using 0.1 cm path-length, a scan rate of 50 nm/min and band width 2 nm. An average of 3 scans for each spectrum were recorded and baseline subtracted (18).

2.3.8 Fluorescence Spectroscopy and Binding Affinities

Purified PhuW was recorded by fluorescence emission spectra on a Perkin-Elmer LS55 luminescence spectrometer with titration of heme or protoporphyrin IX at 25 ˚ C in 20 mM KPB buffer, pH 7.3. To get the binding affinities of purified PhuW with heme or protoporphyrin IX, titrations of diluted PhuW with heme or protoporphyrin IX were recorded by steady state fluorescence emission. The wild type PhuW was used for recording the binding constants in the presence of heme or protoporphyrin IX. The dissociation constants (K_d) were determined by Scatchard plots (19).

2.3.9 Phylogenetic Analyses and Sequence Alignment

Protein sequences similar to the PhuWs from *P. aeruginosa* PAO1 and Campylobacter Jejuni were identified in ExPASy database with BlastP (http://us.expasy.org/cgi-bin/blast.pl). PhuW homologs were manually chosen from the best hits from each BlastP search. Protein sequences homologous to PhuW from *P. aeruginosa* were identified in

GenBank with BlastP. Protein sequences selected were aligned with ClustalW 2.0 program (20). The secondary structure element of PhuW was predicted based on the PhuW sequence and using on PSIPRED predictions at the PSIPRED (Protein Structure Prediction Protein Server) (http://bioinf.cs.ucl.ac.uk/psipred/) (21). The tertiary structure of PhuW was predicted by homology modeling at CPHmodels-2.0 server program at the ExPASy (Expert Protein Analysis System) server (http://us.expasy.org/). The predicted structure was displayed in PyMol.

2.4 Results

2.4.1 Cloning, Expression and Purification of PhuW

The PhuW gene (**Figure 2.2 (A)**) was successfully amplified by PCR and cloned into pET101D Topo vector yielding a construction pET101D/PhuW with PhuW gene fused with a 6-His tag sequence. Positive clones were screened by Xba I/Sac I double digestion (**Figure 2.2 (B)**) of the plasmids. This construct was confirmed by DNA sequencing and transformed into BL21 (DE3) *E. coli* cells for the over-expression of the recombinant PhuW with a C terminal His-tag. Protein expression was induced at OD600 between 0.8-1.0 using 1 mM IPTG and grown for 20 hours at 20 °C. PhuW was purified as a soluble protein by Ni-NTA affinity chromatography (eluted at ~ 30 mM imidazole). After PD-10 column, only one band was detected on SDS-PAGE at ~ 32 kDa (**Figure 2.3 (A)**).

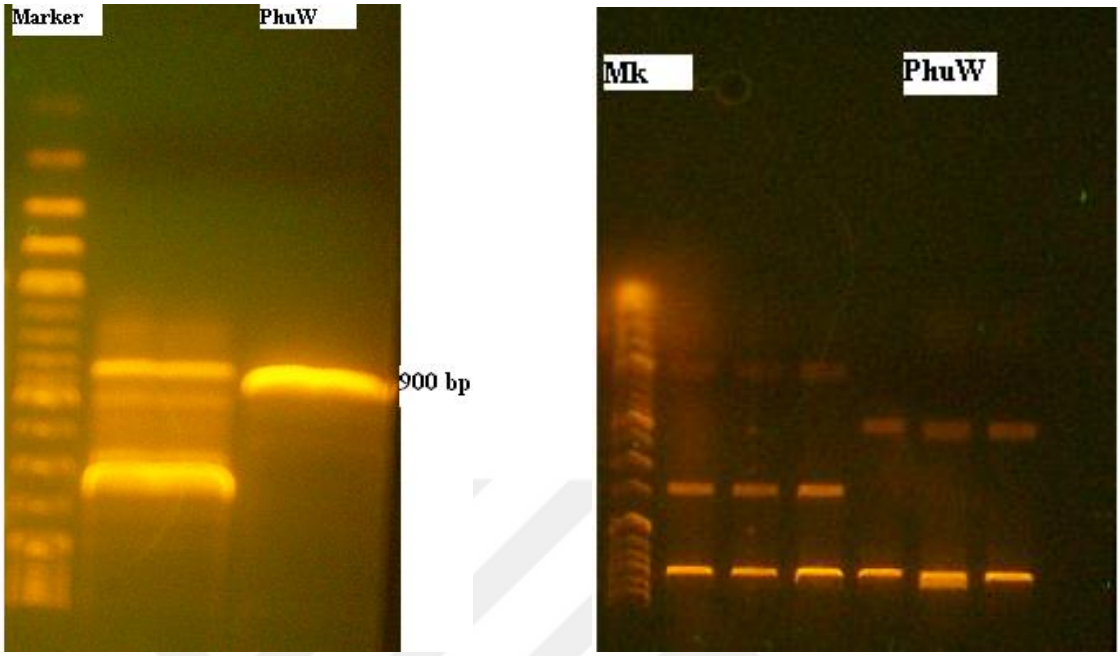

(A) **(B)**

Figure 2.2: Agarose Gel Electrophoresis of PhuW PCR Product. **(A)** Agarose gel indicating the PhuW gene that was successfully amplified as a 900 bp fragment by PCR from genomic DNA of *P. aeruginosa*. **(B)** Agarose gel showing the restriction endonucleases (Xba I and Sac I) double digestion of the DNA constructs pET101D/PhuW. DNA markers from top the bottom: 0.1, 0.2, 0.3, 0.4, 0.5, 0.6, 0.7, 0.8, 0.9, 1.0, 1.2, 1.5, 2.0, 3.0, 4.0, 6.0, 8.0, 10.0 (kb).

2.4.2 Native PAGE and Heme Staining

Native gel electrophoresis is known as non-denaturing gel electrophoresis which is run in the absence of SDS (22). Heme staining and native PAGE were performed to probe if PhuW involves heme and if it binds heme in vitro. Four identical PhuW samples of which two had been incubated with addition of heme at 1:1 molar ratios for 30 min were loaded on a native gel at alternative positions. After electrophoresis, the gel was cut into two

pieces, each containing an untreated PhuW sample and a heme-treated PhuW sample. One of the pieces was stained for protein polypeptides with Coomassie Blue. The other piece was stained for heme as described in the experimental part. The untreated-PhuW samples showed only one band on the native PAGE with Coomassie Blue staining but is negative to heme staining (**Figure 2.3 (B** and **C)**); however, the heme-treated sample showed a broader band (more to the bottom) with Coomassie Blue staining and is positive to heme-staining, suggesting PhuW binds heme in vitro. The non-heme-treated PhuW shows two bands on Coomassie Blue staining, the upper band contains heme-loaded PhuW; the lower band contains heme free PhuW, which can bind heme in vitro.

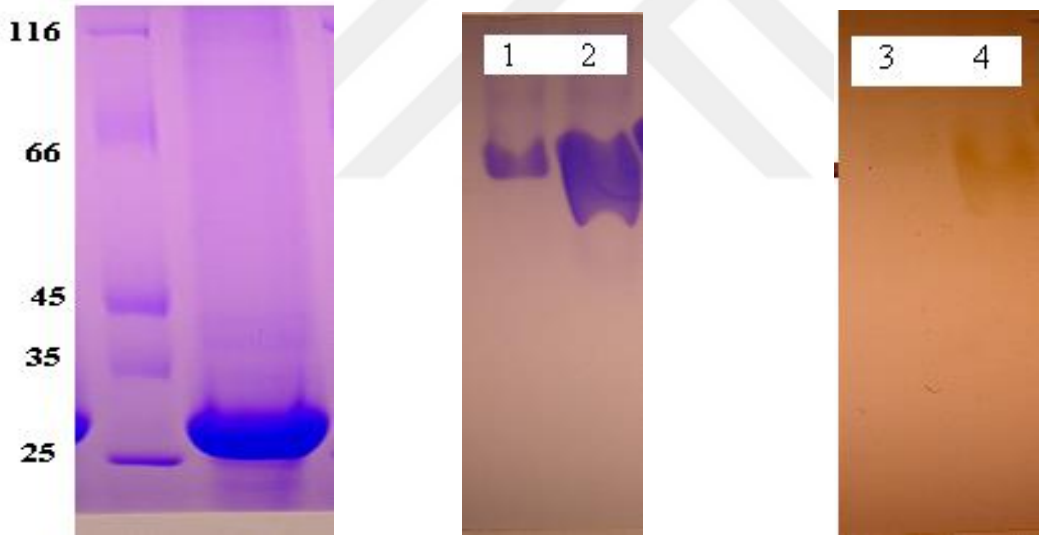

(A) **(B)** **(C)**

Figure 2.3: SDS-PAGE and Native-Page of PhuW. **(A)** SDS-PAGE of the purified PhuW indicates a single band at ~ 32 kDa **(B)** Native-PAGE with Coomassie Blue R-250 staining (lanes 1 and 2). **C)** heme-staining (lanes 3 and 4). Lanes 1 and 3, isolated PhuW; lanes 2 and 4 PhuW loaded with hemin (1:1 mol ratio) for 1 h in phosphate buffer, pH 7.3 before loading gel.

2.4.3 Reconstitution of Holo-PhuW with Hemin

The heme solution were prepared by dissolving hemin or Protoporphyrin IX, freshly prepared into 0.1 M NaOH. Holo-PhuW was obtained by adding small volumes of hemin solution to apo-PhuW protein until a final ratio of 1:1. The heme complex of PhuW was then applied through a PD-10 column to remove non-coordinated heme. Reconstituted PhuW-heme complex concentration was determined by adapting the reported extinction coefficient for PhuW ($_{409}$). The resultant solutions showed a Soret band at ~ 409 nm (**Figure 2.4**), which is clearly distinguishable from the Soret band of free hemin when an aliquot of the hemin solution was added to the PhuW.

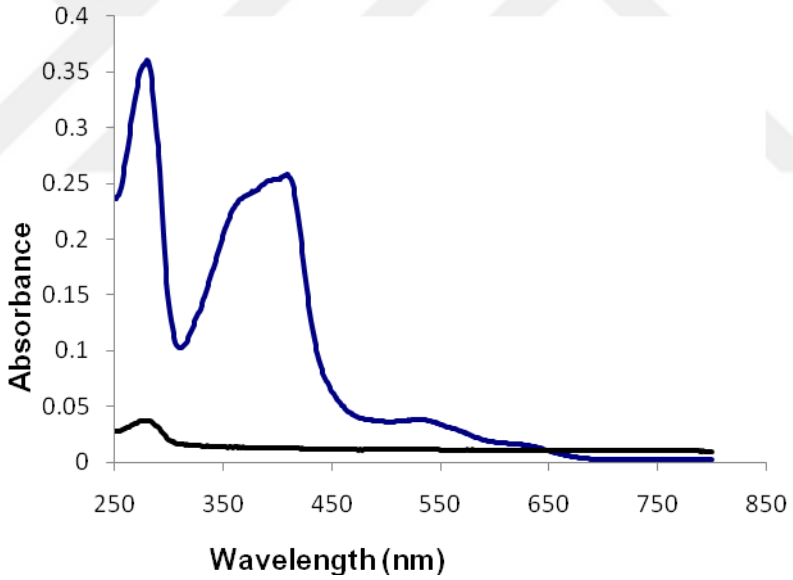

Figure 2.4: UV-vis Spectra of PhuW, apo-PhuW and Holo-PhuW. Comparison of the UV-vis spectra of apo-PhuW (black color, 0.78 µM) and holo-PhuW (blue color, 7.5 µM) in 50 mM potassium phosphate buffer (pH 7.2).

2.4.4 Reduction of PhuW

The UV-visible absorption spectrum of the heme-bound PhuW samples (**Figure 2.5**) show that the heme is oxidized with a Soret maximum at 409 nm, with additional weaker bands at ~ 531 and 627 nm, assignable to β/α metal and charge-transfer band between porphyrin and the high spin Fe(III) (23). Upon reduction of the PhuW using sodium dithionite, (**Figure 2.6**), the Soret band and β, α bands decreased in intensity. The soret band underwent a red shift to ~ 412 nm accompanied by red shifts of the β and α bands (to ~ 530 nm and 572 nm, respectively). Interestingly, the α band increased in intensity at ~ 572 nm, while the CT band at 627 nm disappeared, as well as decrease in intensity at ~ 500 nm (Fe(III) to Tyr CT band) observed. Periplasmic heme protein PhuT decreased in intensity around 500 nm, accompanied by red shifts of the β and α bands (to 560 nm and 589 nm, respectively) and disappearance of the charge transfer band at 624 nm. ChaN function is poorly understood each heme iron is coordinated by a single tyrosine (Tyr-148) from one monomer (28). The apparent dissociation constant of the enzyme-tyrosine complexes in overall reaction could be obtained by spectrophotometric titration at 500 nm in the steady state of the reaction (29). The spectroscopic changes are indicative of a reduction of the ferric heme center with Tyr as an axial ligand (24).

To determine further information for heme coordination, excess imidazole was added to a heme-PhuW solution. The soret band was sharpened and shifted from 409 nm to 412 nm, with an increase in intensity (**Figure 2.7**), accompanied by red shifts of the β and α bands (to 536 nm and 577 nm, respectively. These changes in the UV-vis spectra suggest a 5-

coordinated heme site, with Tyr as a possible axial ligand (25). Large excesses of dithiotheritol (DTT) or sodium ascorbate did not reduce PhuW as judged by UV-vis spectroscopy.

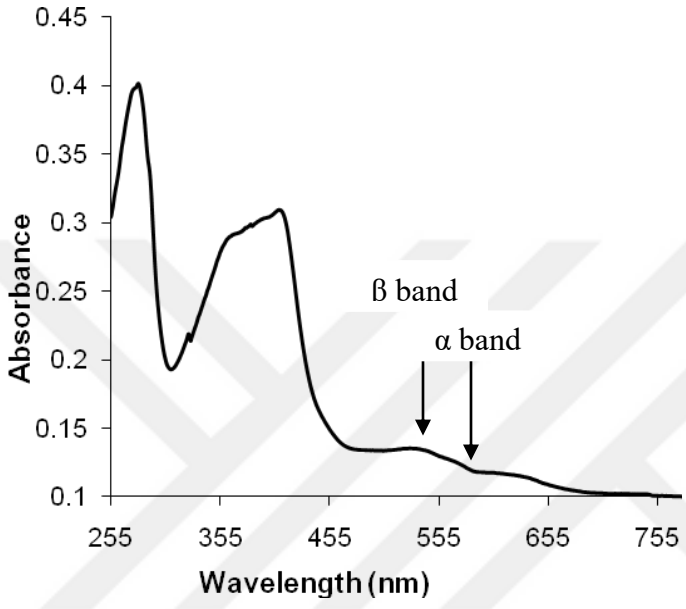

Figure 2.5: UV-Visible absorption spectra of the heme-bound 8.6 µM PhuW, indicates the Soret band at 409 nm (β and α band in 50 mM potassium phosphate buffer, pH 7.3).

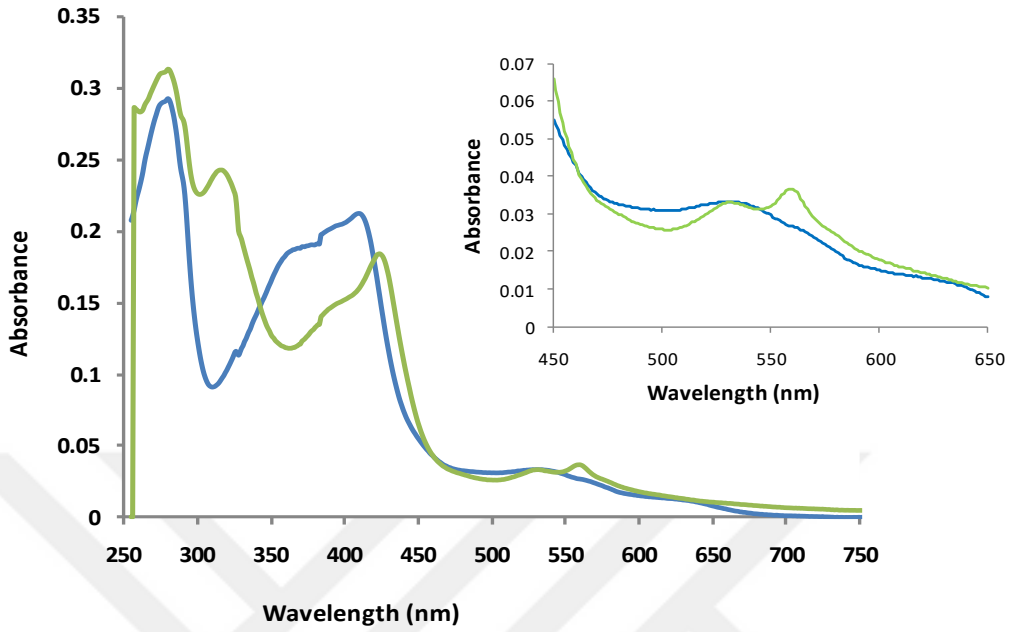

Figure 2.6: UV-Visible spectra of reduction of PhuW by sodium dithionite. Blue color indicates PhuW (6.1 μM) in the presence of 20 mM freshly prepared sodium dithionite, in 20 mM potassium phosphate buffer (pH 7.3).

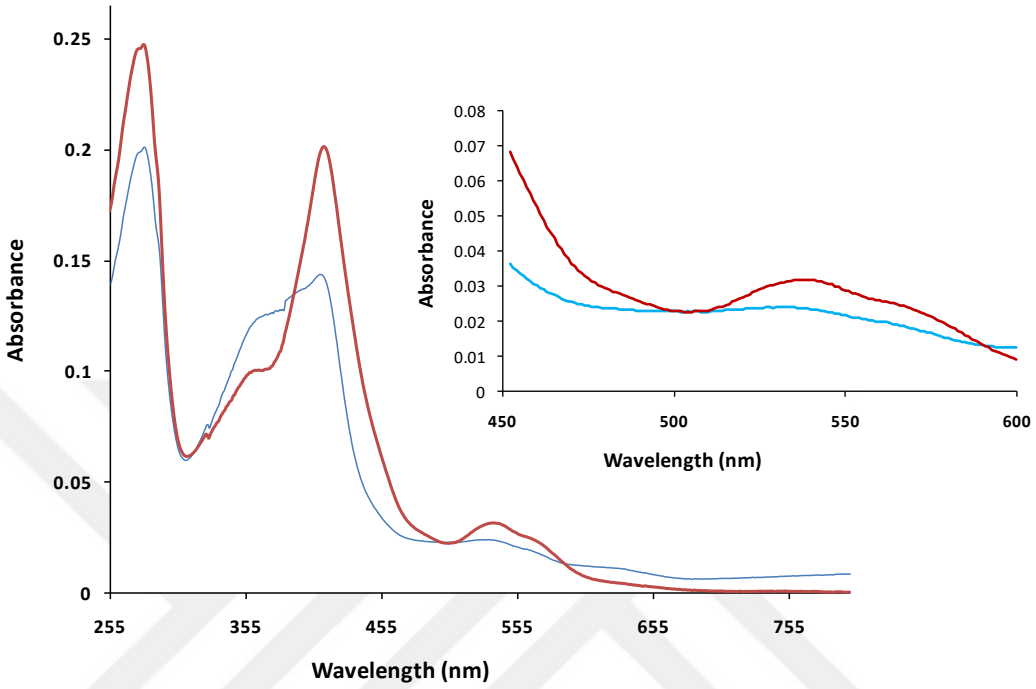

Figure 2.7: PhuW Imidazole Titration. PhuW (4.1 µM, solid line) reacts with large excess of imidazole (0.5 M, dashed line) in 20 mM potassium phosphate buffer (pH 7.3).

2.4.5 Fluorescence Spectra and Binding Affinities with Heme and Protoporphyrin IX

Fluorescence spectroscopy was performed to investigate ligand binding and to detect whether the binding leads to protein conformational change as well as to calculate binding affinities. The cellular actions of a heme begin when the heme (Ligand), L, binds specifically and tightly to its protein receptor, R, on or in the target cell. Ligand-protein affinities is mediated by noncovalent intermolecular interactions (hydrogen bonds, hydrophobic and electrostatic interactions) between the complementary surfaces of ligand

and receptor. Receptor-ligand interaction brings about a conformational change that alters the biological activity of the receptor.

Receptor-ligand binding is described by the equation

Protein (R) + Ligand (L) = Complex;

K_d = [Protein][Ligand]/[Complex]

This binding, like that of an enzyme to its substrate, is based on the concentrations of the interacting components and can be described by an equilibrium constant (K_d). Scatchard analysis (26) of receptor ligand binding allows an estimation of both the dissociation constant K_d and the number of receptor-binding sites. When binding has reached equilibrium, the total number of possible binding sites, B_{max}, is equal to the number of occupied sites, represented by [R], plus the number of occupied or ligand-bound sites, [RL]; that is, B_{max} = [R] + [RL]. The number of unbound sites can be expressed in terms of total sites mines occupied sites: [R] = B_{max} - [RL]. Rearranging to obtain the ratio of receptor-bound ligand to free (unbound) ligand, we get [Bound heme]/ [Free heme] = $1/K_d(B_{max}$-[RL] (27).

In the fluorescence spectra of PhuW, tryptophan fluorescence was monitored at 353 to 354 nm (varying with protein concentration). As indicated in **Figure 2.8**, binding of hemin to the protein results in quenching of the fluorescence at the near UV region. This allows the verification of the 1:1 stoichiometry (**Fig. 2.8** (**C**)) of the heme binding reaction obtained by the aforementioned UV-vis spectroscopy (26). Scatchard analysis **(Figure 2.8 (A)** and **(B)**, **)** gave a linear plot with dissociation constants for heme of 81 nM, respectively, indicting strong binding .

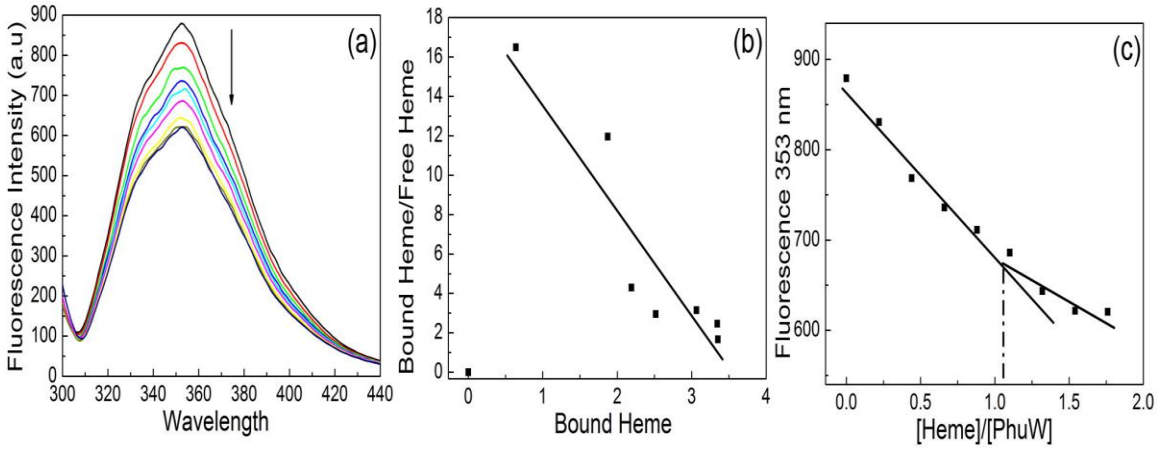

Figure 2.8: Fluorescence spectra of hemin titration to PhuW in 50 mM potassium phosphate buffer (pH 7.2). **(a)** Fluorescent quenching by hemin (374 µM hemin was titrated to a solution of 550 µl PhuW (3.41 µM) with sequence addition of 1 µl heme); **(b)** Scatchard plot for hemin binding to PhuW. **(c)**. Fluorescence intensity of PhuW at 353 nm as a function of the molar ratio of heme vs. PhuW, suggesting a 1:1 stoichiometry.

2.4.6 Far-UV CD Spectrosccopy and Secondary Structure

CD spectroscopy is a valuable method for the characterization of protein structures in solution. This due to the inherent information content of the far-UV CD spectra (between 190-250) which based on the difference in absorption of the left-handed and right-handed circularly polarized light at the protein backbone. The two most prominent peaks in the Far-UV CD spectra of proteins take place at 190 nm (associated $\boldsymbol{\pi}$ $\boldsymbol{\pi}$* transition) and 220 nm (associated with the **n** $\boldsymbol{\pi}$* transition). Other methods are based on the assumption that the spectra are a linear combination of reference spectra for the five secondary structure types (helical conformation, parallel and antiparallel β-sheet, β-turn and random coil). The secondary structure of PhuW was monitored by CD spectroscopy in the far-UV

spectral region (190-250 nm). CD spectroscopy was also performed to determine the effect of heme binding on the secondary structure of PhuW (28). The CD spectra of PhuW are shown in **Figure 2.9**. Both in the absence of and in the presence of heme, PhuW is predominantly α-helical, displaying characteristic minima at 208 nm and 222 nm. Addition of heme to PhuW solution up to 2:1 molar ratio did not lead to any significant changes of the far-UV CD spectrum, suggesting that specific heme binding does not affect the secondary structure of PhuW appreciably.

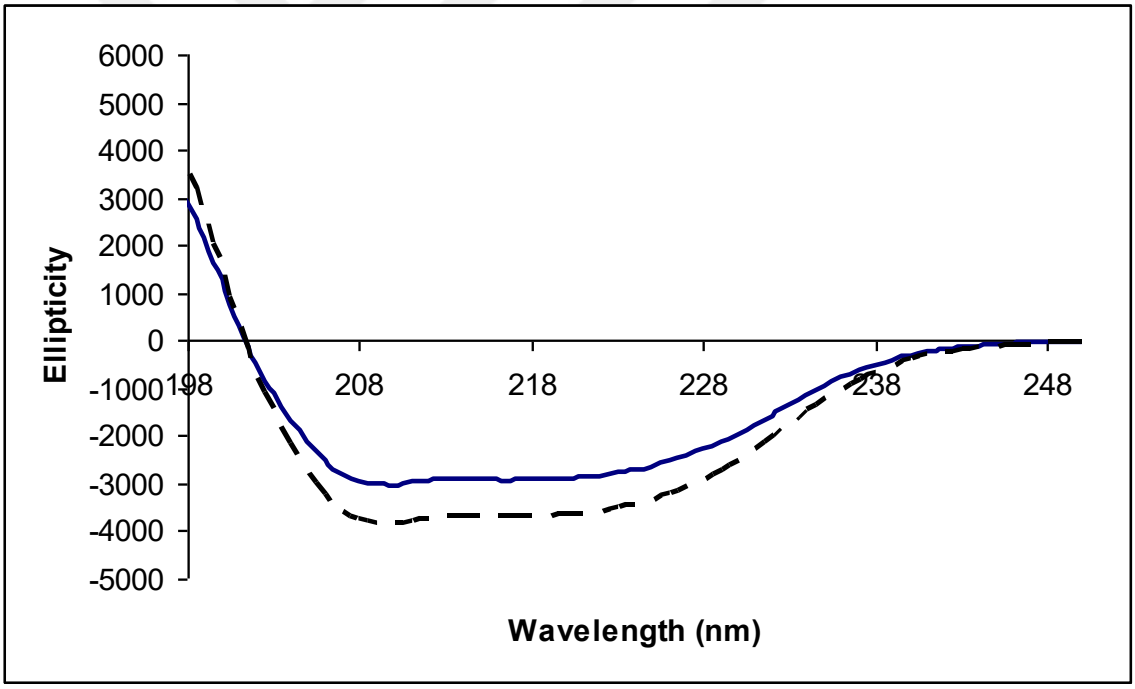

Figure 2.9: Far UV CD spectra of PhuW at 25 ˚ C in 50 mM mM potassium phosphate buffer, pH 7.2. Blue solid line, CD spectra of apo-PhuW (7.2 μM) prepared from cold acid-acetone heme-extraction method. Black dashed line, holo-PhuW (9.1 μM) prepared by addition of 1 equivalent hemein into PhuWsolution. Little change far-UV CD spectra was monitored when titration hemin to the PhuW suggesting hemin binding to the apo-form does not affect significant secondary structure changes of apo-PhuW.

2.4.7 Secondary Structure Prediction and Sequence Analysis

The PSIPRED predicted secondary structure of PhuW is displayed graphically in **Figure 2.10**. The prediction suggest that PhuW contains mainly α-helix with several short β-sheets and a few random coils.

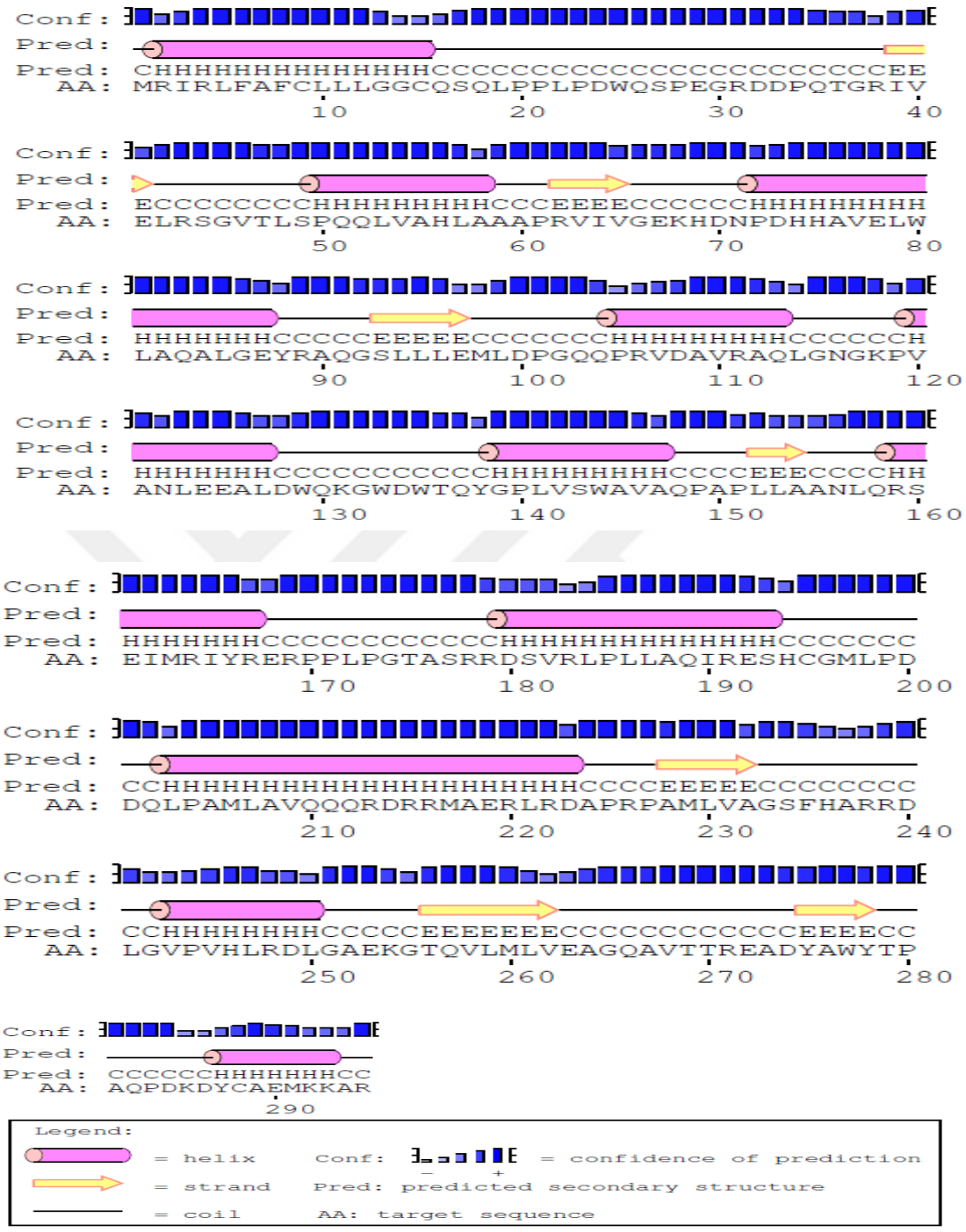

Figure 2.10: The predicted secondary structure of PhuW are indicated above. This prediction is based on PhuW sequence using on PSIPRED predictions at the Protein Structure Prediction Server (http://bioinf.cs.ucl.ac.uk/psipred).

The PhuW homologs found in the BLAST sequence database are derived from several prokaryotes including putative inner membrane lipoprotein [*Escherichia coli* UTI89], iron(III) ABC transporter [*Azotobacter vinelandii* DJ], conserved hypothetical protein [*Serratia odorifera* DSM 4582], Chain X, cofacial heme binding to ChaN which is an iron regulated lipoprotein from *Campylobacter Jejuni*. Sequence homologies between each of the classes are rather low with only 30 to 40% sequence identity. None of these proteins has been biochemically characterized, except for the one from *Campylobacter Jejuni* (shares 30% sequence identity with PhuW) which has been reported recently (29). A structural homology search using ExPASy data base (http://www.expasy.org/) showed that none of these PhuWs, except for ChaN, are yet structurally characterized and do not share any significant homology with any protein. The crystal structure of holo-ChaN reveals that ~ 18% of the heme surface is exposed to solvent. The corresponding value of 23 % is observed for heme bound to hemophore HasA, in which Tyr and His provide axial ligand to a single heme group. Analyses of the sequences (**Figure 2.11**) suggest that the N-terminal sequences are more conserved. One Tyr residue, Tyr166 is found to be strictly conserved in all these sequences. The *C. Jejuni* contains Tyr148, His176, Leu178, Leu186, Leu190, Lys197, Lys189, among which, Tyr148 and His176 are conserved with PhuW from other species. Tyr148 is coordinated to the heme iron in the crystal structure of ChaN (30), suggesting that Tyr166 in *P. aeruginosa* is likely to be a heme ligation residue.

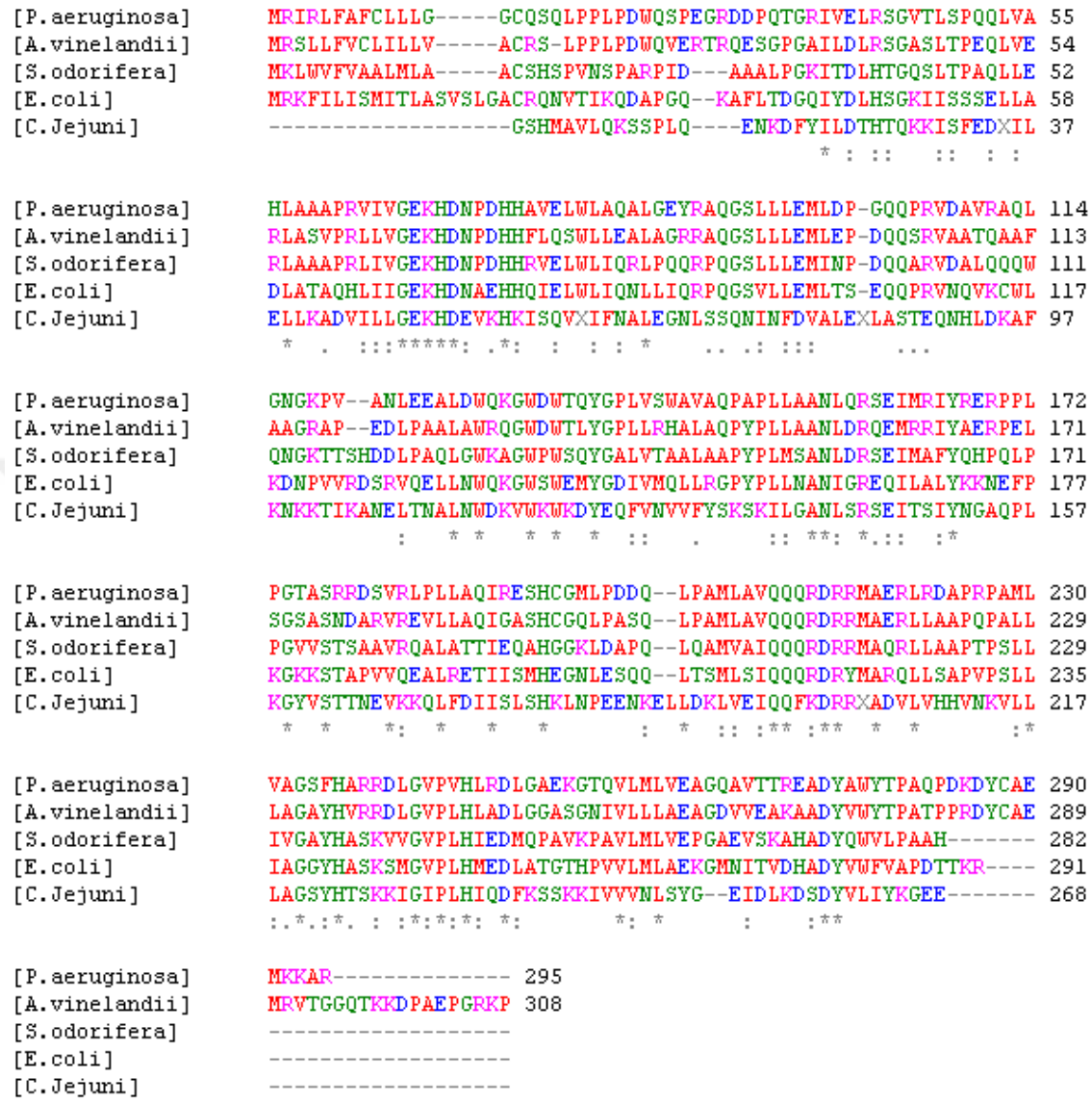

Figure 2.11: Multiple sequence alignment has been performed for PhuW using ClustalW.2.0 program. Fully conserved residues are marked with asterisk, strongly conserved amino acids with colons, and weakly conserved residues with periods. The highly conserved Tyrosine166 is likely heme-ligating ligand.

Homology modeling of the 3D structure of PhuW suggests that it is most likely similar to the crystal structure of ChaN (**Figure 2.13**. Both the homology structure of PhuW and the ChaN structure involve two domains that form a cleft and are linked by a loop and an α-

helix. Domain I in the predicted structure of PhuW comprises of an five-stranded β-sheet sandwiched by nine α-helices. All of the β-sheet strands seem to be parallel to each other. β-1 and β-2 consist of the N terminal and C terminal residues of polypeptide chain. Domain II takes place 3 α-helices (α-6, α-7 and α-8 helixes) arranged in a bundle. In the mixed α-helices, α-7 helix is antiparallel. The conserved heme-binding Tyr residue (Tyr 166 in PhuW and Tyr148 in ChaN) is located on α-6 in domain II.

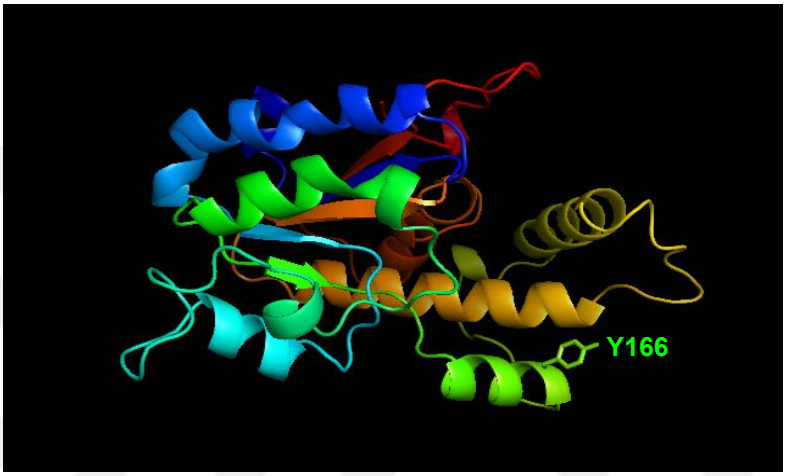

(A)

(B)

Figure 2.12: The Homology Structure of PhuW and Crystal Structure of ChaN. **(A)** The homology structure of PhuW, which was constructed from CPHmodels-3.0 server using PyMOL program. **(B)** The crystal structure of ChaN. Tertiary structure shows the location of heme-coordinating Tyr 148 and N and C termini.

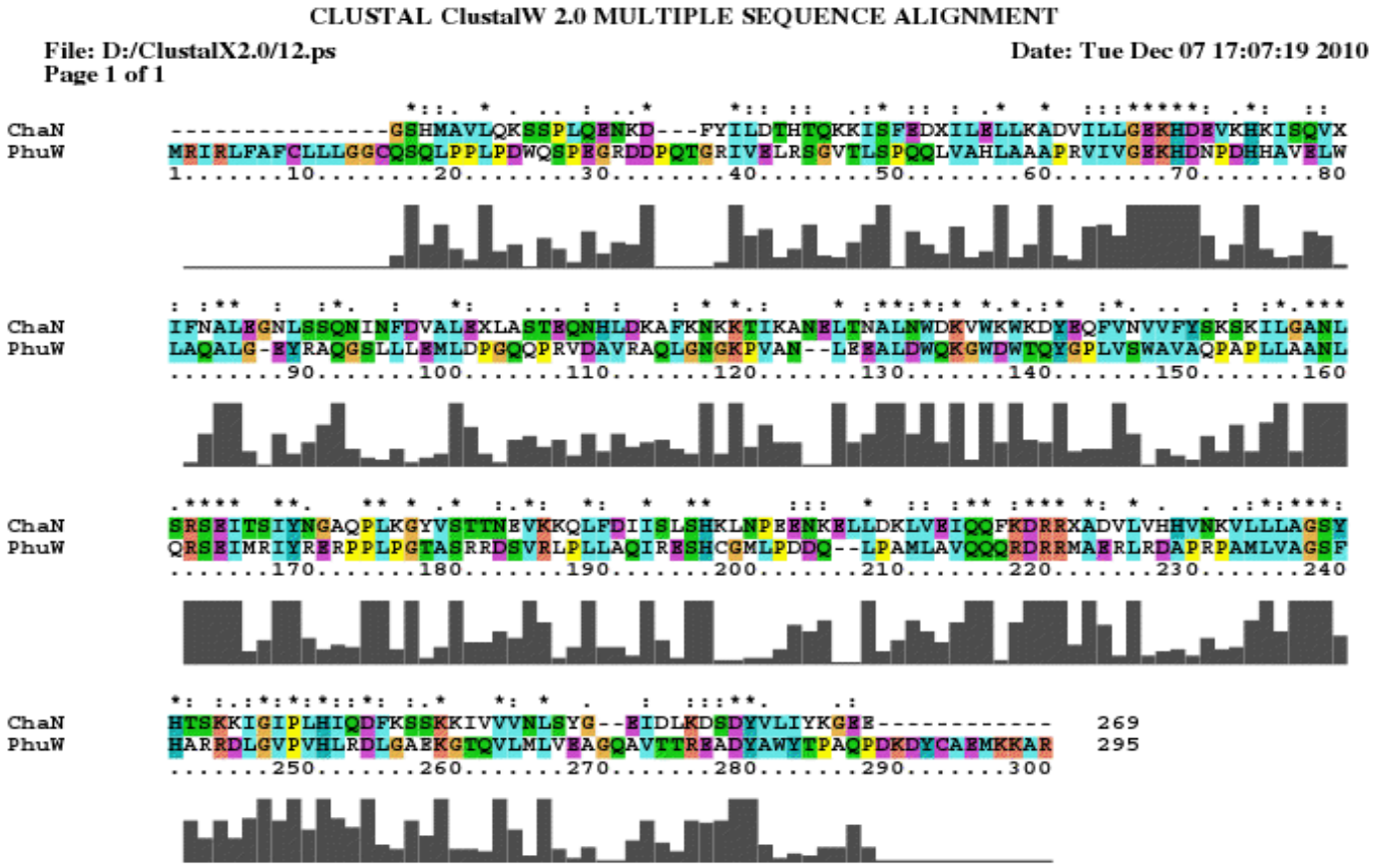

Figure 2.13: Sequence Alignment of PhuW and ChaN. Multiple sequence alignment was aligned for the inner membrane protein PhuW and iron regulated lipoprotein ChaN using ClustalW 2.0 program.

The cytoplasmic protein HemS from *Yersinia enterecolitica* has been indicated to play a role in preventing heme toxicity. In a recent study, PhuS in *P. aeruginosa* has been shown facilitating the transfer of heme to heme oxygenase (80).

The crystal structure of ChaN (**Figure 2.12** reveals that it is composed of a large parallel β-sheet with flanking α-helices and the heme is coordinated by a single tyrosine from one monomer. The EPR spectrum demonstrates that it contains a five-coordinate ferri heme center with a proximal Tyr ligand, while the spectrum at alkaline pH is more complex (30).

2.5 Conclusions

The inner membrane heme transport protein PhuW from *P. aeruginosa* has been cloned and over-expressed in *E. coli*. PhuW binds heme in a 1:1 stoichiometry (K_d ~ 81 nM). CD spectroscopy of Phuw suggests α-helical-rich protein. Formation of heme complex does not affect the secondary structure of the protein appreciably. Heme is 5-coordination in PhuW and Tyr166 is likely the axial ligand.

2.6 References

1. Tong, Y., and Guo, M. (2007) Journal of Biological Inorganic Chemistry **12**, 735-750
2. Andreoni, F., Boiani, R., Serafani, G., Bainconi, I., Dominici, S., Gorini, F., and Magnani, M. (2009) Bioscience Biotechnology and Biochemistry **73 (5)**, 1180-1183
3. Stojiljkovic, I., and Hantke, K. (1994) Molecular Microbiology **13**, 719-732
4. McHugh, J. P., Rodriguez-Quinones, F., Abdul-Tehrani, H., Svistunenko, D. A., Poole, R. K., Cooper, C. E., and Andrews, S. C. (2003) Journal of Biological Chemistry **278**, 29478-29486
5. Crosa, J. H. (1989) Microbiolgy Reviews **53**, 517-530
6. Law, D., and Kelly, J. (1995) Infection and Immunity **63**, 700-702
7. Mizuno, T., and Kageyama, M. (1978) The Journal of Biochemistry **84**, 179-191
8. Ochsner, U. A., Johnson, Z., and Vasil, M. L. (2000) Microbiology **146**, 185-198
9. Cornelis, P. (2010) Applied Microbiology and Biotechnology **86**, 1637-1645
10. Letoffe, S., Redeker, V., and Wandersman, C. (1998) Molecular Microbiology **28**, 1223-1234
11. Alontaga, A. Y., Rodriguez, J. C., Schonbrunn, E., Becker, A., and Funke, T., Yukl, E. T., Hayashi, T., Stobaugh, J., Moenne-Loccuz, P., and Mario, R. (2009) Biochemistry **48**, 96-109
12. Ochsner, U. A., Johnson, Z., and Vasil, M. L. (2000) Microbiology **146 (Pt 1),** 185-198
13. Bradford, M. M. (1976) Analytical Biochemistry **72**, 248-54
14. Laemmli, U. K. (1970) Nature **227 (5259)**, 680-685
15. Enggist, E., Schneider, M. J., Schulz, H., and Thöny-Meyer, L. (2003) Journal of

Bacteriology **185**, 175-183

16. Deniau, C., Gilli, R., Izadi-Pruneyre, N., Letoffe, S., Delepierre, M., Wandersman, C., Briand, C., and Lecroisey, A. (2003) Biochemistry **42**, 10627-10633

17. Lamola, A. A., Asher, I., Muller-Eberhard, U., and Poh-Fitzpatrick, M. (1981) The Biochemical Journal **196**, 693-698

18. Whitmore, L., and Wallace, B. A. (2004) Nucleic Acids Research **32**, 668-673

19. Möller, M., and Denicola, A. (2002) Biochemistry and Molecular Biology Education **30**, 309-312

20. Thompson, J. D., Gibson, T. J., Plewniak, F., Jeanmougin, F., and Higgins, D. G. (1997) Nucleic Acids Research **25**, 4876-4882

21. McGuffin, L. J., Bryson, K., and Jones, D. T. (2000) Bioinformatics **16**, 404-405

22. Elsasser, S., Schmidt, M., and Finley, D. (2005) Methods in Enzymology **398**, 353-363

23. Zelent, B., Kaposi, A. D., Nucci, N. V., Sharp, K. A., Dalosto, S. D., Wright, W. W., and Vanderkooi, J. M. (2004) The Journal of Physical Chemistry B **108**, 10317-10324

24. Ghosh, K., Thompson, A. M., Goldbeck, R. A., Shi, X., Whitman, S., Oh, E., Zhiwu, Z., Vulpe, C., and Holman, T. R. (2005) Biochemistry **44**, 16729-16736

25. Tsai, A. L., Kulmacz, R. J., Wang, J. S., Wang, Y., Van Wart, H. E., and Palmer, G. (1993) The Journal of Biological Chemistry **268**, 8554-8563

26. Nelson, D. L., and Cox, M. M. Lehninger Principles of Biochemistry, Macmillan Press, NY, 2000.

27. Horie, S., Hasumi, H., and Takizawa, N. (1985) The Journal of Biochemistry **97**, 281-293

28. Fatima, S., and Khan, R. H. (2007) The Journal of Biochemistry **142**, 65-72

29. Chan, A. C. K., Lelj-Garolla, B. Rosell, F. I., Pedersen, K. A., Mauk, A. G., and Murphy, M. E. P. (2006) Journal of Molecular Biology **362**, 1108-1119

30. Muro, T., Nakatani, H., Hiromi, K., Kumagai, H., and Yamada, H. (1978) The Journal of Biochemistry 84, 633-640

CHAPTER 3: CLONING, EXPRESSION AND PRELIMINARY CHARACTERIZATION OF THE INNER MEMBRANE HEME TRANSPORT PROTEIN PHUV AND THE OUTER MEMBRANE HEME RECEPTOR PHUR

3.1 Abstract

The membrane components of the heme transport system, the heme receptor PhuR on the outer membrane and the inner membrane heme ABC transporter PhuU (membrane-spanning domain) and PhuV (nucleotide-binding domain) play significant roles in *P. aeruginosa* heme transport process. In this study, PhuR (wild type and a few mutations $PhuR^{F343C}$ and $PhuR^{A527C}$) and PhuUV genes have been amplified by PCR (Polymerase Chain Reaction) and cloned into pET101D vector, respectively. The positive clones were confirmed by enzyme digestion/DNA sequencing. Wild type PhuR, $PhuR^{F343C}$, $PhuR^{A527C}$, and PhuUV were over-expressed in *E. coli* after IPTG induction. $PhuR^{F343C}$, $PhuR^{A527C}$ and PhuV have been purified by Ni-NTA affinity chromatography. PhuV binds heme at 1:1 ratio was revealed by means of UV-Visible and fluorescence spectroscopies, with the binding affinity determined to be (K_d = 564 nM and 107 nM, respectively). To study heme binding/release and heme transport process by Förster Resonance Energy Transfer (FRET), the PhuR mutants were successfully labeled with an Alexa Fluor 488 dye. Heme-free (apo) $PhuR^{F343C}$ and apo-$PhuR^{A527C}$ bind both heme and Protoporphyrin IX in a 1:1 stoichiometry.

3.2 Introduction

Many Gram negative bacterial pathogens have specific outer membrane receptors that sequester heme from free heme or host hemoproteins and deliver it into the periplasmic space via a TonB-dependent system (1). There are several outer membrane receptors that have been identified to date, involving those that bind the secreted siderophores, hemophores, as well as those that directly bind to hemoglobin and the hemoglobin-haptoglobin complex (1). The Phu heme uptake system in *Pseudomonas aeruginosa* consists of an outer membrane receptor PhuR, an inner membrane heme permease PhuU, an ATPase component PhuV, an inner membrane component PhuW, a periplasmic heme binding protein PhuT and a cytoplasmic heme protein PhuS (2). Recently, PhuT and PhuS have been characterized at the protein level (3). In this study, in collaboration with Y. Tong in the lab, PhuR, $PhuR^{F343C}$, $PhuR^{A527C}$, and PhuUV genes were cloned from the genomic DNA of *P. aeruginosa* via PCR (polymerase chain reactions) and, subcloned into pET101D expression vectors. PhuR, the PhuR mutants and PhuUV were over-expressed with the machinery of the T7 RNA polymerase expression system in *E. coli* BL21 cells. The inner membrane heme-bound protein PhuV and the outer membrane heme binding protein PhuR have been purified and characterized at the protein level.

Fluorescence Resonance Energy Transfer (FRET) was first proposed by the German scientist Theodor Förster in the 1940s (4). FRET is a dipole-dipole interaction occurring

between two dye molecules. When the two fluorophores are spatially in close proximity, there is energy transfer between the donor fluorophore and the acceptor fluorophore molecules. The emission energy of a donor fluorophore transfers and excites an acceptor flurorophore (5,6). The donor molecule fluorescence is quenched, and the acceptor molecule is excited (4). There are a few intrinsic fluorophore in proteins (generally aromatic amino acids: tryptophan, tyrosine, and phenylalanine) (7). However, these amino acids makes FRET study of heme uptake system pathway difficult, because their fluorescence quantum yields are weak and less sensitive to the conformational changes (8,9).

3.3 Experimental Procedures

3.3.1 Materials

Pseudomonas aeruginosa PAO1 genomic DNA was purchased from ATCC (Manassas, VA). Directional TOPO Expression kit pET 101 was purchased from Invitrogen (Carlsbad, CA). Oligonucleoties were purchased from Qiagen Operon (Alameda, CA). Enzymes and reagents were purchased from Stratagene and Fermentas. Alexa® Fluor 488 (AF-488) C_5-maleimide was purchased from Invitrogen (Carlsbad, CA). Hemin porcine was purchased from Sigma. Sn (IV) protoporphyrin (IX) dichloride was purchased from Frontier Scientific. Disposable PD-10 desalting columns were purchased from GE Healthcare life sciences. N-lauroyl-sarcosine and n-octyl polyoxyl ethylene (O-

POE) were purchased from Fisher Scientific and Bachem Americas, Inc., respectively. All other kind of chemicals were purchased generally from Fisher and Sigma.

3.3.2 Cloning of PhuR Gene and Construction of Expression Vectors

The gene coding the putative outermembrane heme-binding protein PhuR from bacterial pathogen *P. aeruginosa* was amplified from genomic DNA (PAO1 strain from ATCC) with Polymerase Chain Reaction (PCR). The following oligonucleotides (Qiagen Operon, CA): 5'-CACCATGCCGCTCTCCCCGC-3' (T_m: 70 ˚C) and 5'-GATGTCCCAGACC AGGTTGACCGC-3' (T_m: 70 ˚C) were used as the forward and reverse primers to amplify PhuR gene with stop codon truncated in order to be fused with a downstream His-tag sequence on the vector. The PCR products were then directly cloned into pET 101/D-TOPO® vectors (Invitrogen, Carlsbad, CA) including a built-in V5 epitope and a polyhistidine (6xHis tag) region followed by a stop codon. The PCR cycling conditions were as follows: initial denaturation at 98 ˚C for 30 seconds, 35 cycles consisting of the denaturation step at 98 ˚C for 10 seconds, the annealing step at 72 ˚C for 85 seconds, and the extension step at 72 ˚C for 10 min.

3.3.3 Cloning of PhuUV

The following primers 5'-CACCATGGTGTTGGTCCTCTGGTTGTC-3' (T_m: 69 ˚C) and 5'-ACGGGCGACGATCAGCGGATG-3' (T_m: 68 ˚C)(Qiagen Operon, CA) were

attempted in the PCR to amplify the PhuUV gene. The stop codon for PhuUV was truncated in order to be fused with a downstream His-tag sequence on the vector of pET101/D-TOPO® (Invitrogen, Carlsbad, CA). The PCR cycling conditions for PhuUV were as follows : initial denaturation at 98 ˚C for 35 seconds, 30 cycles consisting of the denaturation step at 98 ˚C for 15 seconds, the annealing step at 60 ˚C for 20 seconds, and the extension step at 72 ˚C for 56 seconds; additional elongation for 10 min at 72 ˚C was performed.

The TOPO cloning products were then transformed into TOP10 One Shot™ competent *E. coli* cells (Invitrogen, CA) and then plated on LB (Luria-Bertani) plate containing 100 μg/ml ampicilin at 37 ˚C overnight. Single colonies on the plate were inoculated in each of 5 ml small-scale culture in LB medium with shaking 220 rpm at 37 ˚C overnight. Plasmid DNA were isolated from these cultures using QIAprep® Spin Miniprep kit (Qiagen, CA) and then screened by restriction enzymes either SacI/XBaI, or PstI (Fermentas, Canada) double digestion followed by agarose gel. Positive plasmid DNAs were confirmed by DNA sequencing at Cornell University Life Sciences Core Laboratories, (Cornell, NJ).

3.3.4 Preparation of Site-Directed Mutants of PhuR

DNA constructs of $PhuR^{F343C}$ and $PhuR^{A527C}$ mutants were successfully amplified using PCR from $PhuR^{WT}$ plasmid DNA aforementioned. Site-directed mutagenesis was performed on the vector pET101/D using a QuickChange site-directed mutagenesis kit

(Stratagene, CA). The forward mutagenic primers: 5'-GCGACCCGCGAGTGCTACTA CCCGATC-3', 5-GATTCGAGAACCTGCAGTG CGGCTACCACATCGAGCC-3', 5'-GGCTTCGGCGCTGTGCCCGGCCAACATC-3'. The entire coding region of the $PhuR^{F343C}$ and $PhuR^{A527C}$ mutants constructs was verified by DNA sequencing. Positive clones were screened by Pst I digestion.

3.3.5 Over-Expression and Purification of PhuR and PhuV

The outer membrane proteins PhuR and mutant PhuRs were over-expressed and produced in BL21 (DE3) *E. coli* cells using expression vector Pet101/D vector following plated on LB plate containing 100 µg/ml ampicilin at 37 ˚C overnight incubation. 5 ml LB medium cultures containing 100 µg/ml ampicilin were prepared by inoculation of a single colony. These cultures were shaken horizontally at 220 rpm at 37 ˚C overnight and used to inoculate large LB medium. Wide-type and mutant PhuRs were induced at 1mM isopropyl-beta-D-thiogalactoside (IPTG) at 20 ˚C for about 18 hours when optical density showed growing the cells between 0.6 and 0.8. The cells were harvested by centrifugation at 3000 rpm for 45 minutes and pellets were collected and stored at -20 ˚C for protein purification. The cells were thawed on ice about 10 min and resuspended in 20 mM potassium phosphate buffer (KPB), pH 7.3 containing 500 mM NaCl, lysozyme (3g/liter), 1 mM PMSF, tiny amount of DNase and RNase, and 1% (w/v) N-lauroyl-sarcosine and subsequently sonicated on ice for one min, alternating the power between on (0.5 second) and off (1.5 sec); this step was repeated 3 more times for a total of 3 min. The solution was centrifuged at 18, 000 rpm for 45 min. The part of supernatant was separated and the cell pellets were solubilized in 20 mM KPB, 500 mM NaCl, 1 mM

PMSF and 7% octyl-polyoxyethylene (O-POE), and then sonicated on ice for 10 min. After a 1 hour incubation on a rotator at room temperature, the solution was centrifuged before loading the supernatant onto Ni-NTA affinity column. From this point, all buffers contained 1%O-POE. Proteins were rinsed with a linear gradient of 10-1000 mM imidazole concentration in 20 mM KPB, 100 mM NaCI and 1% O-POE. PhuR proteins were eluted at 100 mM imidazole analyzed by SDS-PAGE. Fractions including PhuR were concentrated using an Amicon Ultra concentrator (Milipore, MA). PD-10 desalting column was used to change the buffer as necessary (3).

Wild-type recombinant PhuV was over-expressed in BL21 (DE3) *E. coli* cells and purified by Ni-NTA metal affinity chromatography. The cell pellet was resuspended in 50 mM KPB (pH 7.3), 300 mM NaCl, 1 mM PMSF, 1mM benzamidine, 2.5% DM (n-Decyl-beta-D-maltopyranoside), tiny amount of DNase and RNase, and then sonicated on ice. The PhuV protein fractions were collected by centrifugation at 18, 000 rpm for 45 min. Supernatant was loaded onto Ni-NTA affinity column. The column was pre-equilibrated with 50 mM KPB, 300 mM NaCl , and 0.1% DM. Proteins was eluted at 50 mM imidazole concentration.

3.3.6 Labeling of PhuR Mutants with AF-488 C_5-Maleimide

To perform fluorescent measurements, PhuR mutant proteins were purified and labeled with AF-488 maleimide (Chemical structure shown in Fig. 3.1). Fluorescent labeling was done using a standard procedure for the thiol-reactive probes conjugation to $PhuR^{A527C}$

(10). Briefly, 59.55 µM PhuR^{A527C} mutant protein was dissolved in 250 µl 20 mM KPB, 100 mM NaCl, 1% O-POE buffer (pH 7.3) at room temperature. At this pH point, the thio groups in the PhuRs are efficiently nucleophilic so that they could react with AF-488 maleimide. A 10-fold molar excess of reducing agent TCEP (tris-(2-carboxyethyl) phosphine) was added to the solution to reduce the sulfide bonds in the proteins to liberate free thiols (11). In a typical labeling reaction, 1-10 mM AF-Alexa 488 maleimide stock solution in DMSO was freshly prepared (molar extinction coefficient 71,000cm^{-1}M^{-1} at 494 nm). A 10-fold molar excess of AF-488 maleimide was added dropwise to the protein solution as it was in stirring. The reaction of the maleimide double bond with thiol group in the protein was allowed to proceed overnight on ice. A 60-fold molar excess of glutathione was added to consume excess thio-reactive reagent, subsequently passing through PD-10 gel filtration column (12).

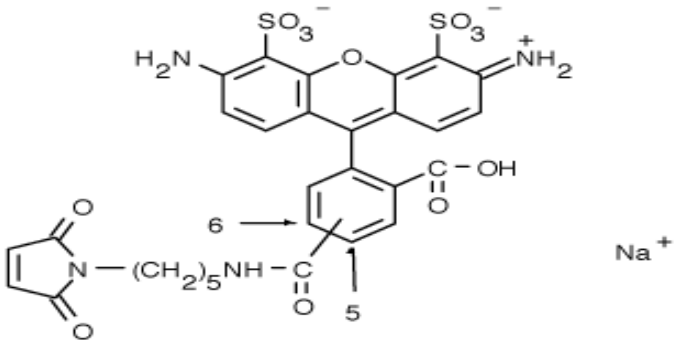

Figure 3.1: Chemical structure of AF-488 maleimide.

3.3.7 Fluorescence Spectroscopy and Binding Affinities

To determine the binding affinities between PhuRs, PhuV and heme, addition of heme or protoporphyrin IX to purified apo-PhuRs and PhuV were carried out at 25 ˚C in 20 mM KPB, 100 mM NaCl, pH 7.3 and measured by steady state fluorescence emission spectra on a Perkin-Elmer LS55 luminenscence spectrometer with excitation wavelengths at 495 nm. The dissociation constants (K_d) were calculated by Scatchard plots as forementioned (13).

3.3.8 Heme Staining

Heme staining of proteins separated by sodium dodecyl sulfate (SDS)-15% polyacrylamide gel electrophoresis was carried out with *o*-dianisidine (Sigma) as the substrate as described previously (14).

3.3.9 Reduction of PhuV

Reduction of PhuV was recorded by UV-vis spectroscopy in 20 mM sodium phosphate buffer (pH 7.3) on a Perkin-Elmer (Lamda 25) spectrophotometer. The reduced form of PhuV (1-10 μM) was obtained by addition of sodium dithionite (20 mM).

3.3.10 Reconstitution of PhuV with Hemin and UV-visible Spectroscopy

In order to determine if the PhuV protein can bind heme and to probe if it can bind Fe-free protoporphyrin IX, titration experiments were performed in 20 mM sodium phosphate buffer (pH 7.3) and recorded by UV-vis spectroscopy. All the experiments were performed with 1-cm cuvettes on a computer controlled Perkin Elmer Lambda 25 spectrometer at 25 ˚C. UV-visible spectra after addition of heme (208 μM) to PhuV were monitored immediately and at different time intervals. The range used for the spectrum was 800 –250 nm. To calculate the amount of holo-PhuV in the sample the absorbance at the Soret band was measured. All heme solutions were freshly made in 0.1 M NaOH and the molar absorptivity used was ε_{385} value of 58,440 $M^{-1}cm^{-1}$ (15).

3.4 Results and Discussion

3.4.1 Cloning of PhuR and PhuUV Genes

PhuR (2.3 kb) and PhuUV (1.7 kb) genes were successfully amplified by PCR (**Figure 3.2**) from *Pseudomonas aeruginosa* genomic DNA and cloned into pET101D Topo vectors. DNA construct were excised from the agarose gel and extracted with MinElute™ Gel Extraction Kit (Qiagen, CA).

3.4.2 Pst I Digestion of PhuR- and PhuUV-pET101/D Plasmids

Positive clones were screened by PstI digestion (**Figure 3.3**) of the plasmids. PstI has a single-cut on the PhuR and PhuUV at 1577/1573 and 1519/1515, respectively; it has also a single-cut on the pET101/D vector at 1489/1485.

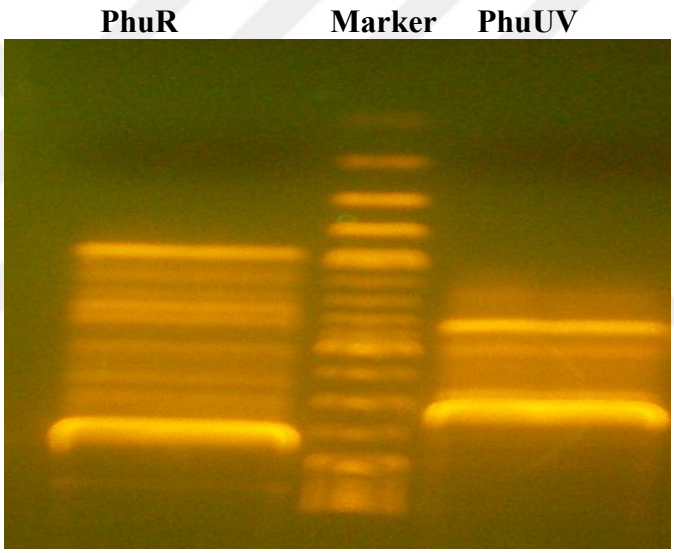

Figure 3.2: Agarose Gel of PhuR and PhuUV. Agarose gel indicating the PhuR and PhuUV genes that were successfully amplified by PCR. DNA markers from top the bottom: 0.1, 0.2, 0.3, 0.4, 0.5, 0.6, 0.7, 0.8, 0.9, 1.0, 1.2, 1.5, 2.0, 3.0, 4.0, 6.0, 8.0, 10.0 (kb).

The new constructs are named as pET101D/ PhuR that are confirmed by PstI enzyme digestion (6 kb and 1.9 kb DNA fragments in Figure 3.3) and as pET101D/PhuUV that

are confirmed by PstI digestion (6 kb and 1.4 kb DNA fragments in Figure 3.3). These constructs were also confirmed by DNA sequencing at CLC.

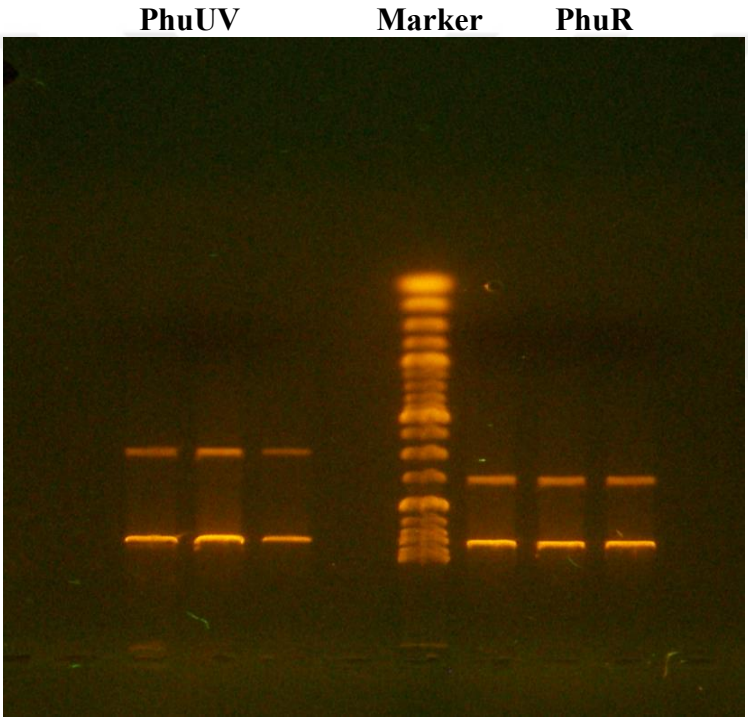

Figure 3.3: PstI digestion of PhuR-pETt101/D and PhuUV-pET101/D. Agarose gel showing the restriction endonuclease (PstI) digestion of PhuR-pETt101/D and PhuUV-pET101/D. DNA markers from top the bottom: 0.1, 0.2, 0.3, 0.4, 0.5, 0.6, 0.7, 0.8, 0.9, 1.0, 1.2, 1.5, 2.0, 3.0, 4.0, 6.0, 8.0, 10.0 (kb).

3.4.3 Purification of Wild-type PhuR and PhuV

In order to characterize their heme binding properties in vitro, the outer membrane protein PhuR and the inner membrane protein PhuV were overexpressed in *E. coli* BL21 (DE3) cells. Overexpressed PhuR or PhuV protein represented the major band on SDS Polyacrylamide gels in extracts of *E. coli* BL21 (DE3) transformed with the vectors. Wild-type PhuR and PhuV were purified as a 70 kD and as a 30 kD protein, respectively, in agreement with the predicted molecular weights for each proteins (**Figure 3.4**).

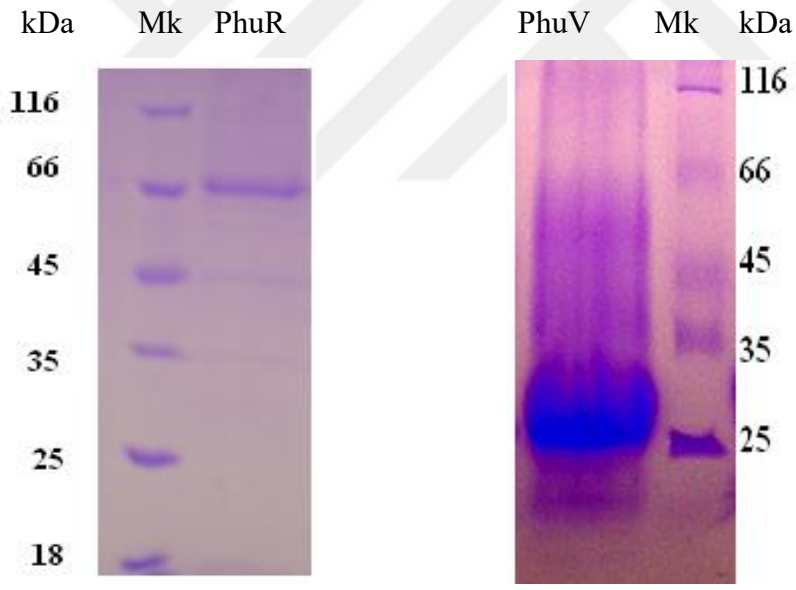

Figure 3.4: SDS-PAGE of Purified PhuR and PhuV. SDS-PAGE of the purified PhuR (left); and PhuV proteins (right).

3.4.4 Mutagenesis Study of PhuR

In many organisms, the study of developmental processes has made remarkable advances

with the use of mutants, which are excellent tools to elucidate protein functions. With the help of mutants, it has been possible to identify and clone numerous genes involved in many different aspects of heme bacterial proteins development. Phe 343, Ala 527, and Ala 742, which are located on the surface of the PhuR homology model, were chosen for mutagenesis to cys (Figure 3.5) residue for site-specific dye labeling. In order to have an effective FRET, the donor and acceptor molecules must be in close proximity (Typical 10-100 Å). The distances of the cys residues of PhuR^{F343}, PhuR^{A527} and PhuR^{A742} to G118, a site close to the predicted heme-binding site in phuR, are measured as 17.7 Å, 15.9 Å and 21.5 Å, respectively.

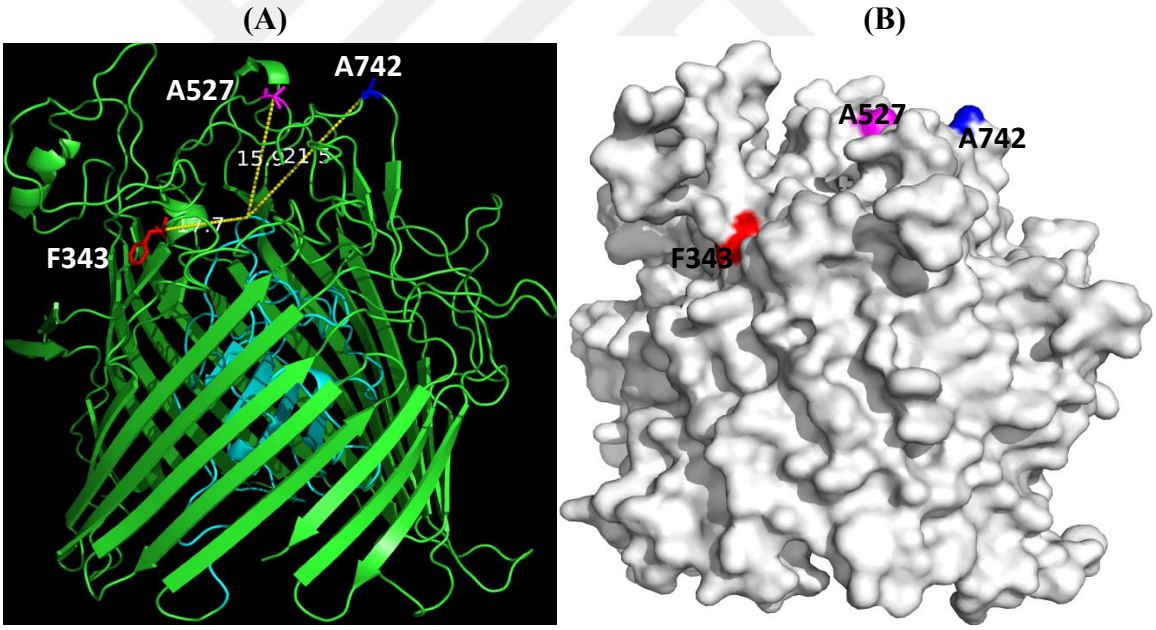

Figure 3.5: Homology model of PhuR mutant Proteins. Structure model of PhuR was indicated in cartoon (A) and sphere (B) model. F343, A527 and A 742 labeled in red, magenta and blue color, respectively. PhuR mutant proteins homology model were constructed with SWISS-MODEL (11,12).

3.4.5 Cloning and Purification of Mutant PhuR Proteins

The PhuR variants F343C, A527C, and A742C plasmids were cloned by PCR using QuickChange site-directed mutagenesis kit (Stratagene, CA). Positive clones of the PhuR mutants were subjected to restriction by PstI enzyme (**Figure 3.6**) and DNA sequencing.

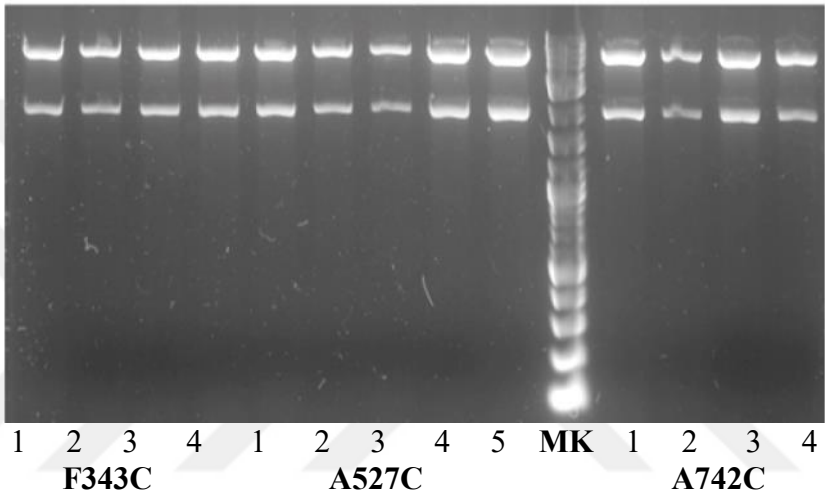

Figure 3.6: PstI digestion of PhuR mutants, F343C, A527C, and A742C. DNA markers from top to the bottom: 10.0, 8.0, 6.0, 4.0, 3.0, 2.0, 1.5, 1.2, 1.0, 0.9, 0.8, 0.7, 0.6, 0.5, 0.4, 0.3, 0.2, 0.1 (kb).

The mutant proteins of PhuR were purified by using a Ni-NTA affinity column. The purified proteins were analyzed by SDS-PAGE method and stained by Commassie Blue.

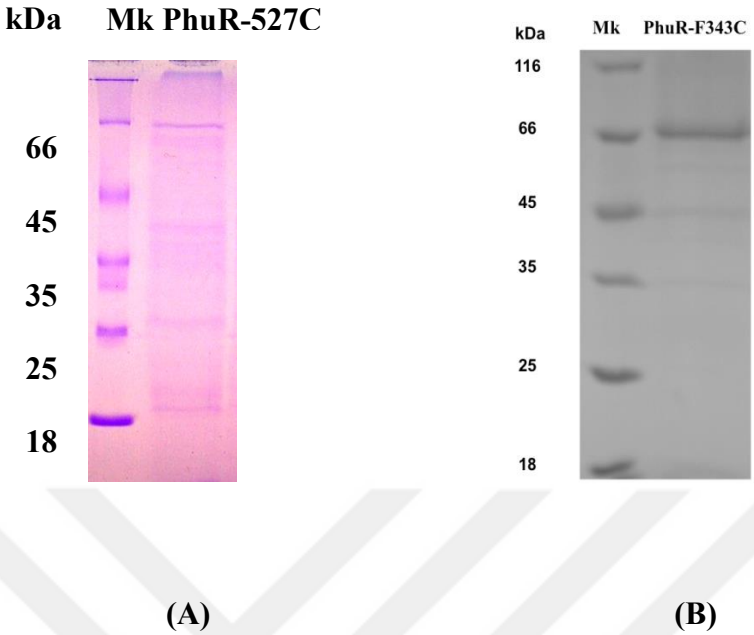

Figure 3.7: SDS-PAGE gel picture of PhuR^{A527C} (**A**); PhuR^{F343C} (**B**).

3.4.6 FluoresceMnce Spectra and Binding Affinities of Heme/Protoporphyrin to PhuR and PhuV

Fluorescence spectroscopy was applied to study ligand binding and to detect conformational changes as well as to calculate binding constants. Fluorescence spectroscopy measurements were carried out on a Perkin-Elmer LS55 luminenscence spectrometer at 25 ˚C in 20 mM KPB, 100 mM NaCl (pH 7.3). To determine the heme binding affinities of purified PhuR^{F343C}, PhuR^{A527C} and PhuV proteins, titrations of diluted protein samples with the addition of heme or protoporphyrin IX were monitored by steady state fluorescence emission. The mutant PhuR proteins A527C (**Figure 3.8**), F343C (**Figure 3.9**) and the inner membrane protein PhuV (**Figure 3.10**) bind heme or protoporphyrin IX at a 1:1 ratio. The dissociation constants (K_d) were calculated by the

method of Scatchard plots for PhuR^{A527C} of 108 nM, PhuV of 107 nM and PhuR^{F343C} heme and protoporphyrin IX of 69 nM and 181 nM, respectively. (13).

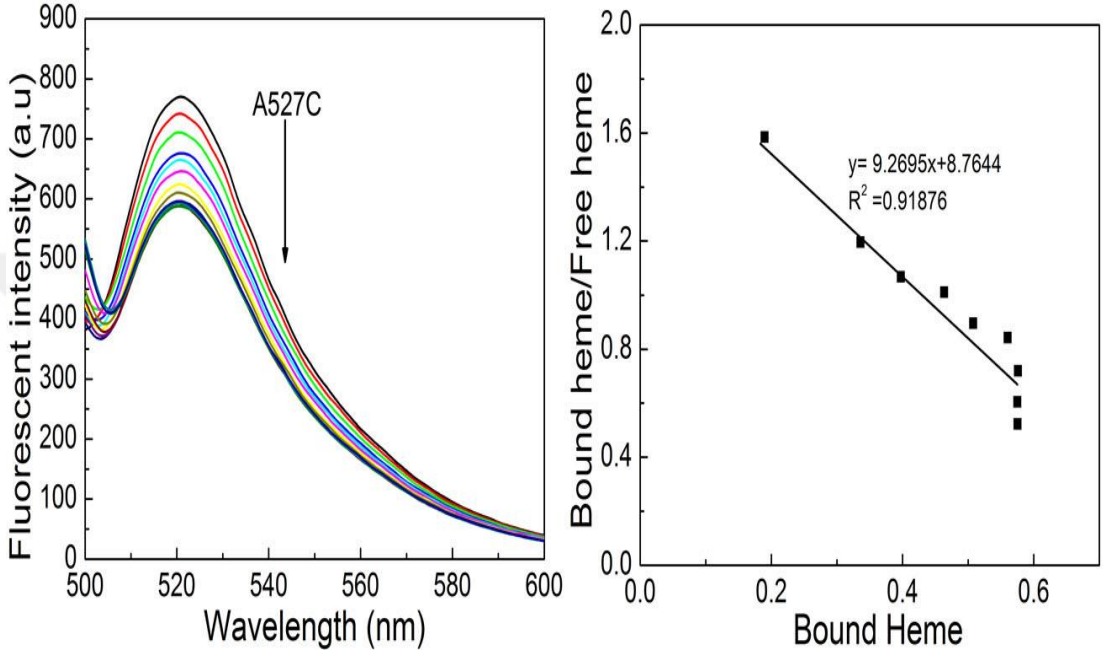

Figure 3.8: Fluorescence Heme Titration to PhuR^{A527C}. Fluorescence spectra of titration of aliquots of heme (0.155 µM to 1.39 µM) to the outer mutant membrane protein PhuR^{A527C} (0.568 µM) in 20 mM sodium phosphate buffer, pH 7.3, in the presence of 1% O-POE detergent.

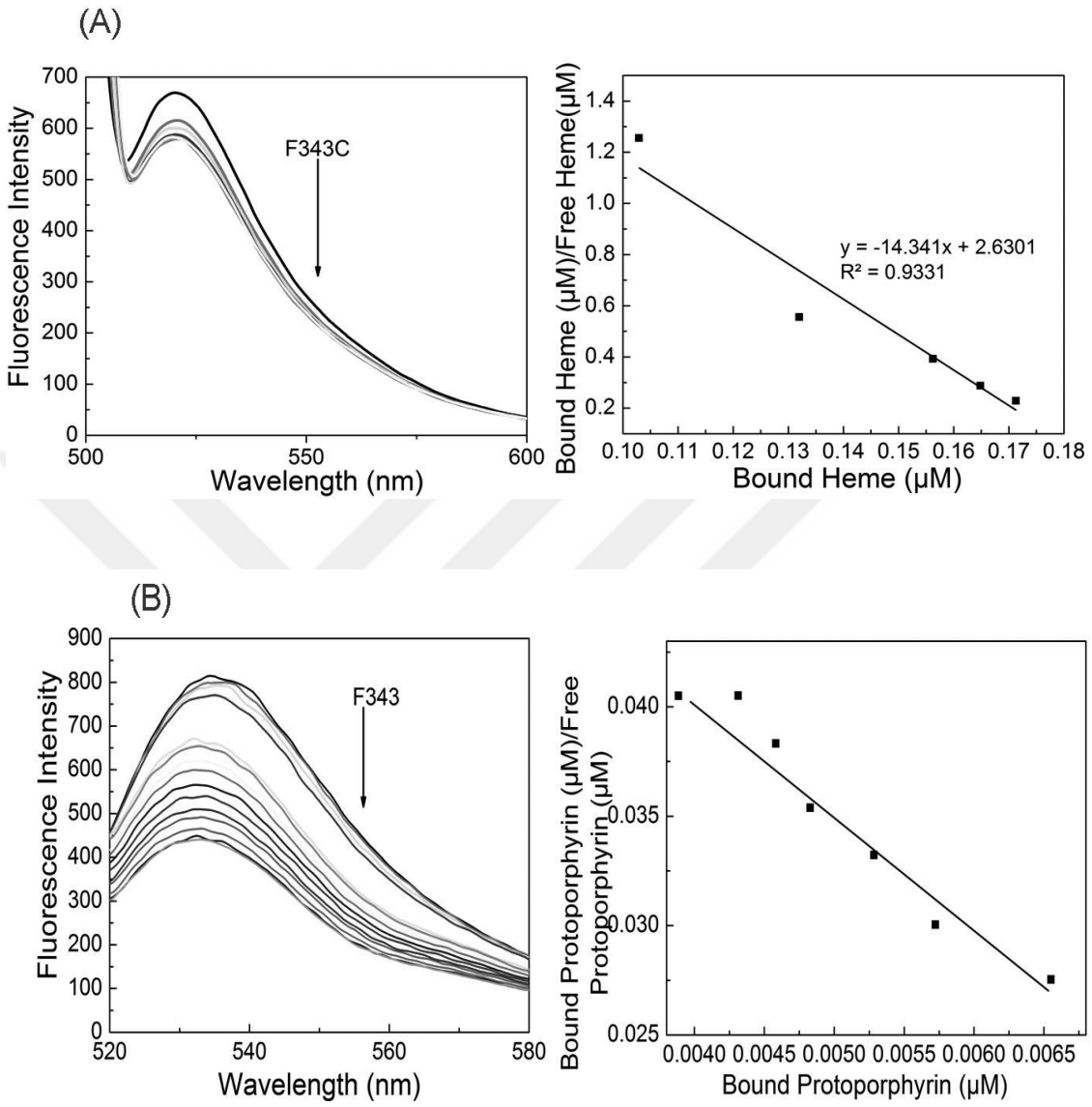

Figure 3.9: (A) Fluorescence Heme/Protoporphyrin Titration to PhuR^{F343C}. Fluorescence spectra of titration of aliquots of heme to 0.172 μM PhuR^{F343C} in 20 mM sodium phosphate buffer (pH 7.3), 1% O-POE at 25 ˚C. Fluorescent quenching by 222 μM hemin (from 0.40 μM to 4.44 μM) was added to a solution of 550 μl PhuR in 20 mM KPB, 100 mM NaCl (pH 7.3) with increasing increments of 1 μl); **(B)** Fluorescence spectra of titration of aliquots of protoporphyrin IX (58.6 μM, prepared in 0.1 NaOH) to 0.089 μM PhuR^{F343} (from 0.105 μM to 1.05 μM, at 0.105 μM increments).

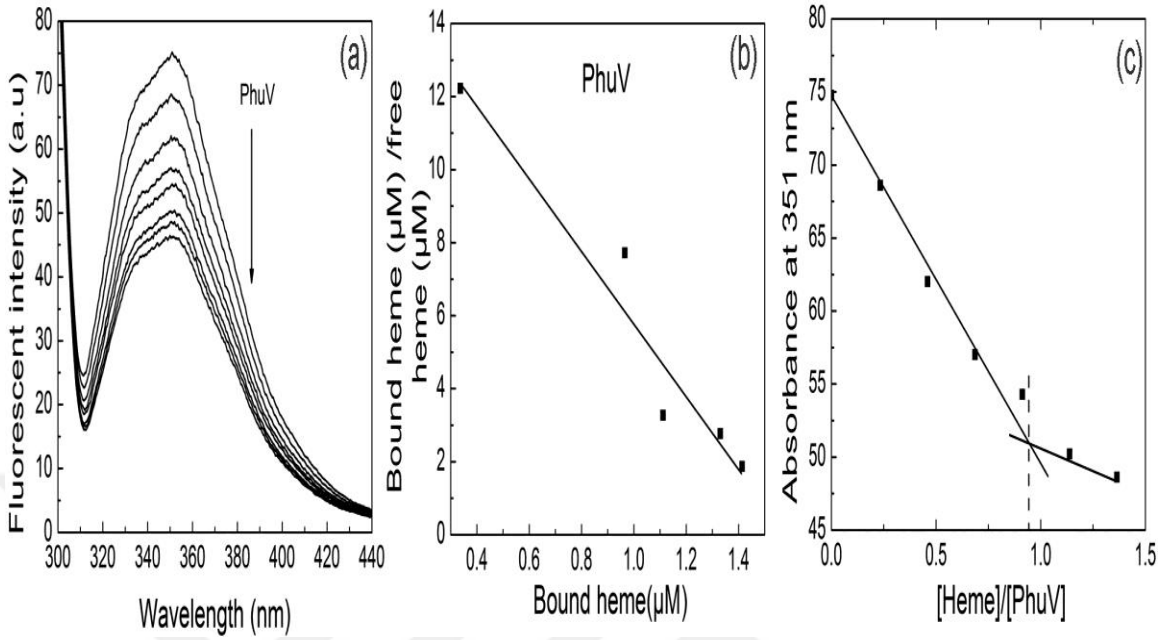

Figure 3.10: A) Fluorescence Heme Titration to PhuV. Fluorescence spectra of 201.5 μM heme aliquots titrated to inner membrane heme protein PhuV (1.566 μM) in 20 mM KPB, 100 mM NaCl (pH 7.3). **B)** Scatchard plot analysis of PhuV binding heme. **C)** PhuV saturation curve at a 1:1 ratio.

3.4.7 Heme Staining Assay

To determine whether PhuV binds heme, heme staining assay was performed. After heme treatment, samples were subjected to native-PAGE. The gels obtained from native-PAGE were subjected to heme staining with *o*-dianisidine or to protein staining with Coomassie Blue R-250 as described (16). The untreated PhuV samples showed one band on the native PAGE with Coomassie Blue staining but is negative to heme staining (lanes 1 and 4 in **Figure 3.11**). The heme-treated samples (lanes 2, 3) migrated slower than the untreated sample but are positive to heme staining (lanes 5 and 6 in **Figure 3.11**), indicating that the PhuV binds heme in vitro.

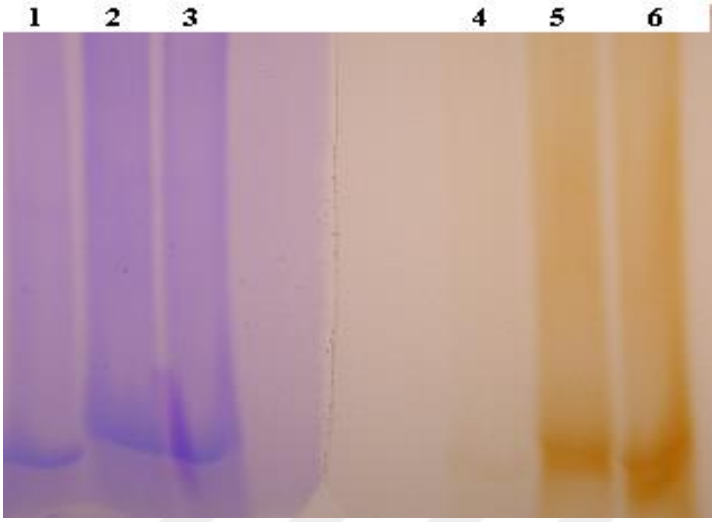

Figure 3.11: Heme Staining Assay. PhuV was purified by Ni-NTA affinity chromatography and subjected to Native-PAGE. Gels were stained with Coomassie Blue R-250 (Lanes 1,2,3) and for heme (lanes 4,5,6). Lanes 1 and 4, isolated PhuV; lanes 2,3 and 5,6, 1, 56 μM PhuV incubated with 242 μM heme at 1:1 ratio and 1:2 in 20 mM KPB, 100 mM NaCl (pH 7.3) buffer for 30 minutes.

3.4.8 Electronic Spectroscopy and Reduction of Heme Transport Proteins

The purified PhuV protein (**Figure 3.12**) displays a sharp band with maxima at ~ 412 nm in UV-visible spectrum, characteristic of Soret band for a hemoprotein, as well as three additional weaker broad bands at ~ 530, 567, and 643 nm, attributable to β/α bands and ligand to metal charge-transfer (LMCT) band between the porphyrin and high-spin Fe (III) (18), respectively. The UV-vis spectrum resembles hemoproteins with His as axial ligand, e.g. myoglobin (19). In order to further probe this, imidazole was added to the sample. After adding even large excess of imidazole to the PhuV solution (**Figure 3.13**),

little change to the Soret band was observed. Only minor increase in intensity of the β/α and CT bands was observed. This is in contrast to those observed for PhuT and PhuW, where addition of imidazole causes major changes to the soret bands and β/α and CT bands. This data provides strong support for histidine imidazole as the axial ligand to the ferric heme iron in PhuV (17,18).

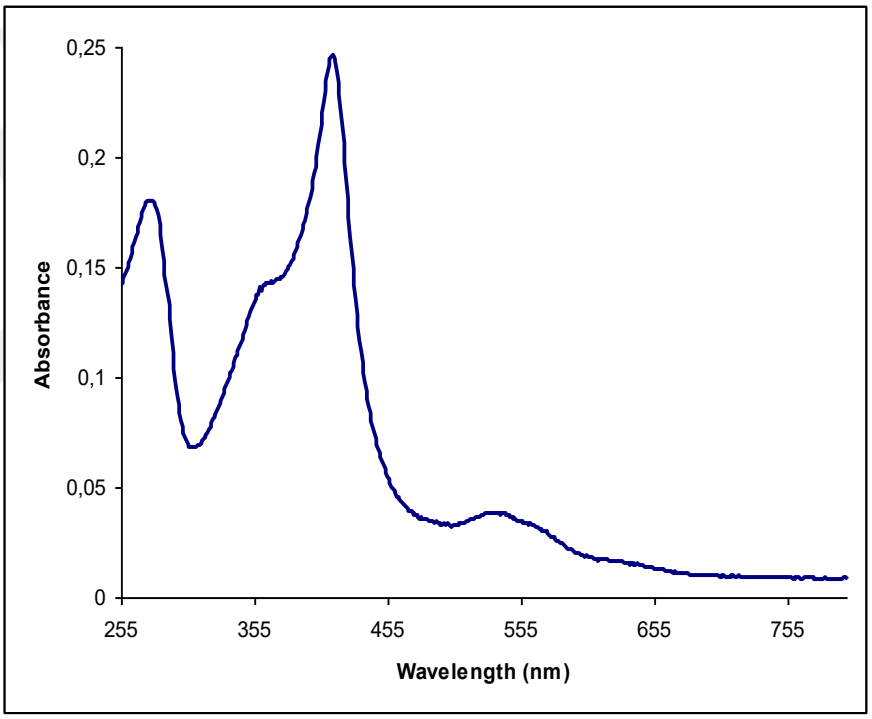

Figure 3.12: UV-Visible absorption spectra of 12.7 µM the holo-PhuV (solid line), indicates the Soret (β band, α band and charge-transfer band in 20 mM potassium phosphate buffer (pH 7.3)).

Sodium dithionite was added to generate reduced PhuV spectra. The spectrum of PhuV with its heme iron in the Fe^{+2} oxidation state, obtained upon addition of sodium dithionite

(Figure **3.14**), shows the Soret band at 425 nm, the α band and β bands at 528 and 560 nm, respectively and no absorption near 643 nm, as expected. The β band decreases and the α band increases in intensity. This spectral behavior implies that the PhuV heme is, when oxidized, in a high spin configuration (19).

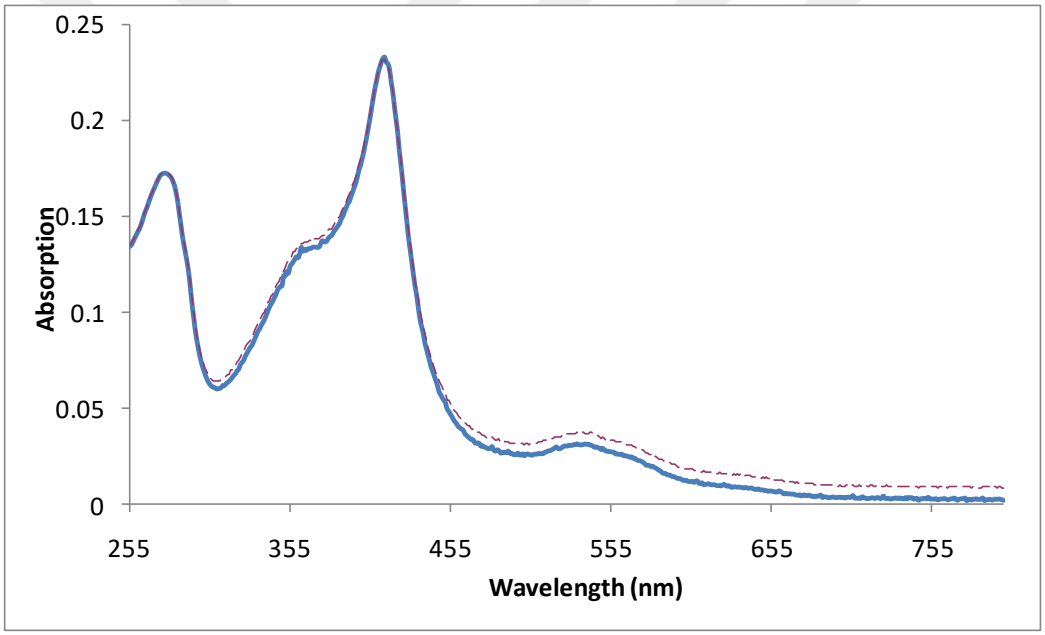

Figure 3.13: PhuV Imidazole Titration. PhuV (12 µM, solid line) reacts with large excess of imidazole (0.5 M, dashed line) in 20 mM KPB 100 mM NaCI pH 7.3.

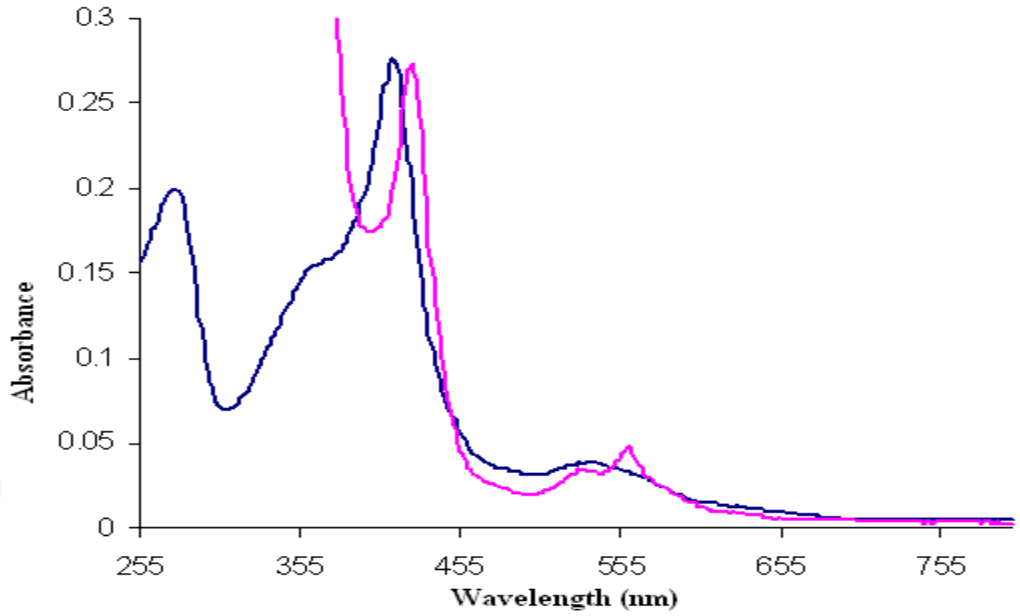

Figure 3.14: UV-vis spectra of reduction of 14.2 µM PhuV by sodium dithionite (20 mM) in 20 mM KPB, 100 mM NaCI pH 7.3.

3.4.9 Reconstitution of PhuV with Hemin

PhuV and hemin were used to reconstitute holo-PhuV in vitro. Upon reconstitution with heme the Soret maximum of the heme-PhuV complex occurs at 412 nm at pH 7.3, with visible bands at 530,567 and 643 nm (**Figure 3.15**). PhuV at a concentration of 7.5 µM was treated by incubating at room temperature for at least for 30 min with 10 µM hemin. The absorbance spectra were monitored from 200 to 800 nm by subtracting the absorption due to hemin in the buffer. The sprectra of hemin at similar identical conditions were also monitored. The PhuV showed strong absorption peaks at 412 nm while the maximum absorbance of free hemin was at 392 nm (**Figure 3.15**). To determine the protein-hemin stoichiometry and binding constant, successive aliquots (1 µl) of 208 µM hemin were added to the sample cuvette, which contained 8.9 µM PhuV,

and a reference cuvette containing 20 mM potassium phosphate buffer alone. Spectra were monitored 10 min after the addition of each hemin aliquot. Spectrophotometric titration indicated a progressive increase in absorbance at 412 nm (**Figure 3.16**). Plotting the spectral changes observed at 412 nm versus the hemin concentration yielded a saturation curve, and the data showed that the PhuV binds hemin in a 1:1 stoichiometry (**Figure 3.18**). Scatchard analysis gave a linear plot with a binding affinity (K_d = 564 nM) (**Figure 3.17**).

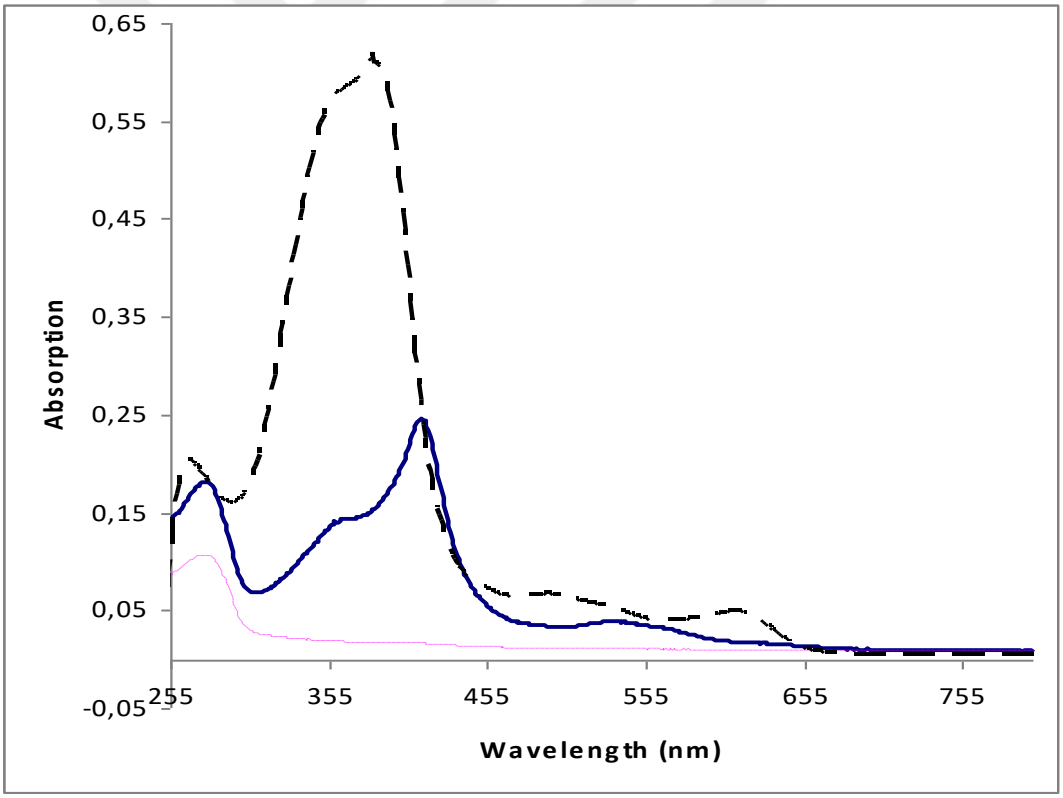

Figure 3.15: UV-Vis Absorption Spectra of apo- and holo-PhuV. UV-Vis absorption spectra of 10.4 µM hemin alone (dashed line), 7.5 µM inner heme permeases protein PhuV (dotted line), and hemin-PhuV complex (solid line) in 20 Mm KPB, 100 mM NaCI pH 7.3.

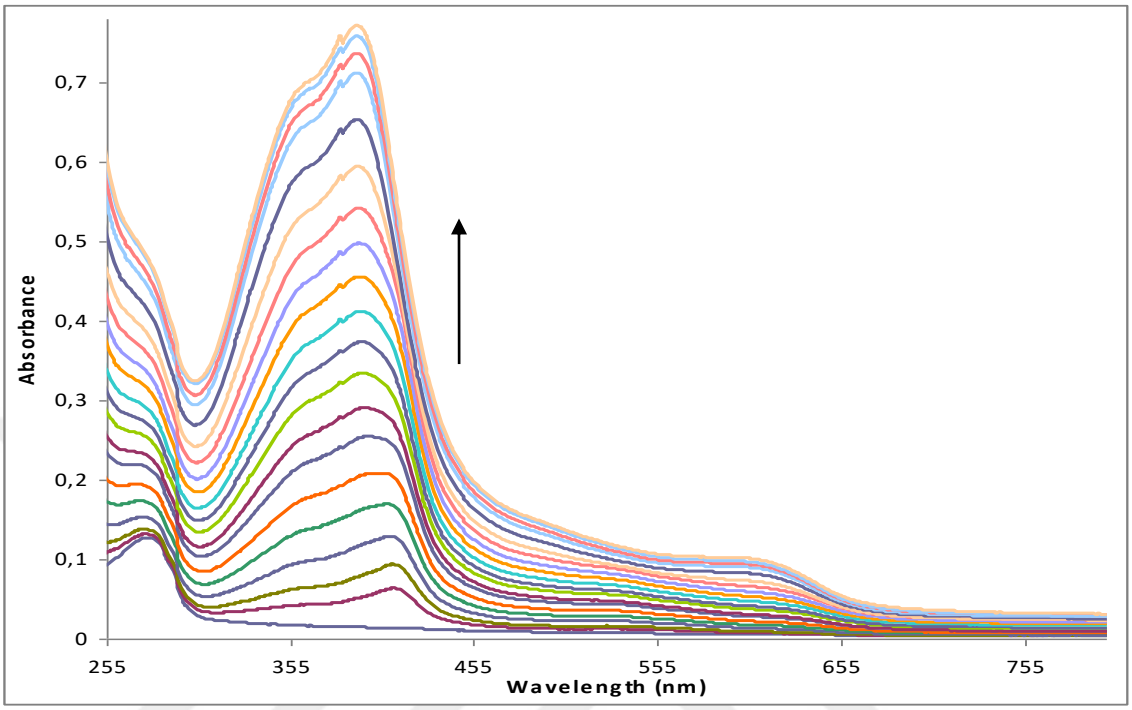

Figure 3.16: UV-Vis absorption Heme Titration to PhuV. UV-Vis absorption spectra showed that the maximum absorbance of free hemin 392 nm shifts to a longer wavelength (412 nm) after binding of PhuV to hemin. The absorption spectra of increasing concentrations of 208 µM hemin added to PhuV protein (8.9 µM) were acquired.

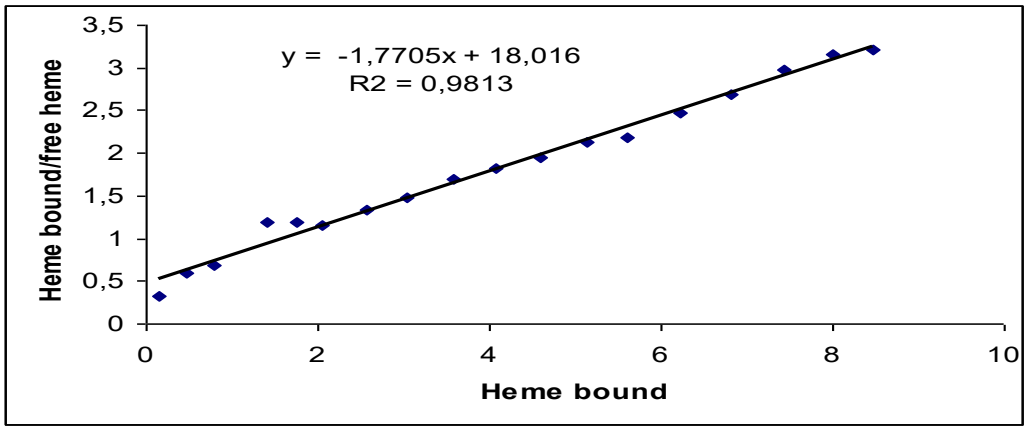

Figure 3.17: Scatchard plot analysis of 8.9 µM PhuV binding heme in 20 mM KPB, 100mM NaCI pH 7.3.

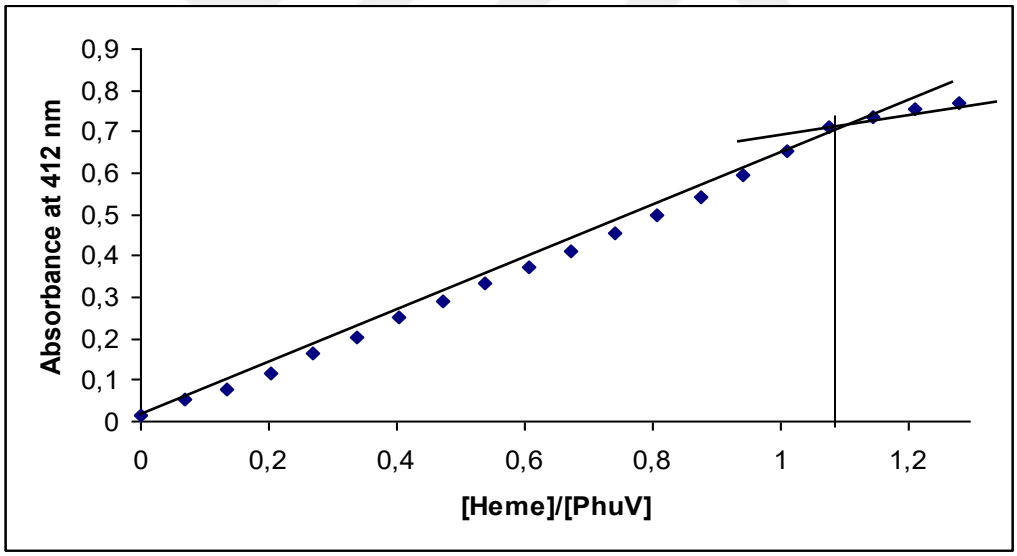

Figure 3.18: PhuV Saturation Curve. Plotting the spectral changes observed at 412 nm versus the hemin/PhuV concentrations yielded a saturation curve at a 1:1 ratio in 20mM KPB, 100mM NaCI, pH 7.3.

Table 3.1: The summary of the characterization of heme binding proteins encoded in the *P. aeruginosa* heme-uptake *phu* locus

Protein name	Cellular location	Molecular mass (Da)	pI	Homologues (% identity)	Putative function
PhuR	Outer membrane	84 600	5.7	*Y. enterocolitica* HemR (24)	Heme receptor
PhuU	Inner membrane	33 600	9.7	*Y. enterocolitica* HemU (48)	Heme permease
PhuV	Inner membrane	27 500	6.2	*Y. enterocolitica* HemV (45)	ATPase component
PhuW	Inner membrane	32 900	7.3	*C. jejuni orfW* product (27)	Unknown

3.5 Discussion

The ability to transport heme is an significant virulence factor for bacterial pathogens as heme is the most abundant source of essential iron in many pathogenic bacteria or mammalian host (20,21). Iron uptake system from host heme plays an important role in bacterial infections (22). Furthermore, heme is a potent pro-oxidative, promoting the light-dependent formation of reactive oxygen species that can cause non-enzymatic redox reactions (23).

The successful cloning and the biochemical characterization of the inner membrane protein PhuW, ATPase component PhuV and the mutation of PhuR proteins from *P. aeruginosa* have been provided more information about the understanding of the PhuRSTUVW heme transport system (Table 3.1) and other similar bacterial heme transport system. Recently, PhuT and ShuT have been purified and characterized as a heme binding protein with crystal structures (24). Also the crystal structure of heme bound ChaN, a PhuW analogue in *Campylobacter jejuni* was expressed and purified. ChaN exhibited a clear growth defect using heme as the sole iron source. Additional homologues of ChaN are found in many pathogenic bacteria (25).

The heme staining assay results showed that PhuW and PhuV can be produced as apo- and heme bound modes. Heme staining of proteins have displayed that PhuW and PhuV can bind hemin in vitro.

The ChaN, an iron-regulated lipoprotein from *Campylobacter jejuni,* has been reported recently as the first member of its lipoprotein family to bind heme specifically. PhuW shares 30% sequence identity with ChaN (25). Our investigation showed that these two heme transport proteins share some similarities, i.e., they both bind one heme per protein molecule in vitro. ChaN has a low spin, five-coordinated ferriheme center with a proximal Tyr ligand. This proximal tyrosine ligand is Y148 in ChaN and most likely to be Tyr 166 in PhuW, as suggested by the multiple sequence alignment studies and the homology structure.

PhuV also binds heme, as revealed by UV-vis and fluorescent titration (**Figure 3.16** and **Figure 3.10**, respectively). Scatchard analysis gave a linear plot with a binding affinity (K_d) (**Figure 3.17**) determined. The affinities (dissociation constant K_d) of hemin to PhuV were estimated to be 564 nM by UV-vis and 107 nM by fluorescence, respectively. The measured K_d difference between the two methods is ca 5-fold. The lower binding constant obtained from UV-vis titration is probably due to the overlap of the soret bands of the bound heme and the free heme in the system. In the fluorescence titration, free heme is not interfere with the protein Trp signal. Thus the binding constant obtained from the fluorescence titration is more reliable.

PhuR binds heme at 1:1 ratio with affinity at submicromal range. K_ds in the micromolar range have also been reported for the *serratia marcescens* TonB-dependent heme receptor HasR and the *Porphyromonas gingivalis* outer membrane heme receptor HmuR (26). The affinity of *P. damselae* subsp. *piscicida* HutB to the ligand appears weaker than the periplasmic hemin binding protein PhuT of *P. aeruginosa*.

These biochemical features for the bacterial outer membrane heme receptor PhuR, inner membrane protein PhuW and ATPase component PhuV will contribute to a better understanding of the bacterial heme transport pathway.

3.6 Conclusions

PhuR, PhuUV genes were amplified by PCR and cloned into pET101D vectors and confirmed by DNA sequencing. PhuR and its variants, and PhuV were purified by Ni-NTA affinity chromatography. PhuR and its variants bind heme at 1:1 ratio with high affinity. In vitro study indicates that PhuV also binds heme in a 1:1 stoichiometry with affinity at submicromolar. Histidine appears to be the heme ligands in PhuV.

3.7 References

1. Eakanunkul, S., Lukat-Rodgers, G. S., Sumithran, S., Ghosh, A., Rodgers, K. R., Dawson, J. H., and Wilks, A. (2005) Biochemistry **44**, 13179-13191

2. Wandersman, C., and Stojiljkovic, I. (2000) Current Opinion in Microbiology **3**, 215-220

3. Ochsner, U. A., Johnson, Z., and Vasil, M. L. (2000) Microbiology **146 (1)**, 185-198

4. Tong, Y., and Guo, M. (2007) Journal of Biological Inorganic Chemistry **12**, 735-750

5. Didenko, V. V. (2001) Biotechniques **31 (5),** 1106-1121

6. Han, F., Luo, Y., Ge, N., and Xu, J. (2008) Acta Biochimica et Biophysica Sinica **40**, 934-942

7. Ota, N., Hirano, K., Warashina, M., Andrus, A., Mullah, B., Hatanaka, K., and Taira, K. (1998) Nucleic Acid Research **26**, 735-743

8. Lakowicz, J. R. Principles of Fluorescence Spectroscopy, Springer, NY, 2008

9. Ray, K., Szmacinski, H., and Lakowicz, J. R. (2009) Analytical Chemistry **81**, 6049-6054

10. Ammor, M. S. (2007) Journal of fluorescence **17**, 455-459

11. Haugland, R. P. Handbook of Flourescent Probes and Research Chemicals, Molecular Probes, Eugene, 1996

12. Getz, E. B., Xiao, M., Chakrabarty, T., Cooke, R., and Selvin, P. R. (1999) Analytical Biochemistry **273**, 73-80

13. Benkova, B., Lozanov, V., Ivanov, I. P., Todorova, A., Milanov, I., and Mitev, V. (2008) Journal of Chromatography B **870**, 103-108

14. Galbraith, R. A., Sassa, S., and Kappas, A. (1985) Journal of Biological Chemistry **260**, 12198-12202

15. Laemmli, U. K. (1970) Nature **227 (5259)**, 680-685

16. Deniau, C., Gilli, R., Izadi-Pruneyre, N., Letoffe, S., Delepierre, M., Wandersman, C., Briand, C., and Lecroisey, A. (2003) Biochemistry **42**, 10627-10633

17. Thomas, P. E., Ryan, D., and Levin, W. (1976) Analytical Chemistry **75**, 168-176

18. Nemykin, V. N., Rohde, G. T., Barrett, C. D., Hadt, R. G., Sabin, J. R., Reina, G., Galloni, P., and Floris, B. (2010) Inorganic Chemistry **49**, 7497-7509

19. Franzen, S., Bailey, J., Dyer, R. B., Woodruff, W. H., Hu, R. B., Thomas, M. R., and Boxen, S. G. (2001) Biochemistry **40**, 5299-5305

20. Takeuchi, F., Kobayashi, K., Tagawa, S., and Tsubaki, M. (2001) Biochemistry **40**, 4067-4076

21. Iverson, T.M., Arciero, D.M., Hsu, B.T., Logan, M.S.P., Hoope A.B., and Rees, D.C. (1998) Nature Structural & Molecular Biology **5**, 1005-1012

22. Ghosh, K., Thompson, A. M., Goldbeck, R. A., Si, X., Whitman, S., Oh, E., Zhiwu, Z., Vulpe, C., and Holman,T. R. (2005) Biochemistry **44** (50), 16729-16736

23. Guo, M., Harvey, I.,Campopiano, D. J., and Sadler, P. J.(2006) Angewandte Chemie International Edition **45**, 2758-2761

24. Skarr, E. P., and Schneewind, O. (2004) Microbes and Infection **6**, 390-397

25. Ho, W. W., Li, H., Eakanunkul, S., Tong, Y., Wilks, A., Guo, M., and Poulos, T. L. (2007) The Journal of Biological Chemistry **282**, 35796-35802

26. Chaija, M. (2008) Songklanakarin Journal of Science and Technology **30**, 47-53

27. Burkhard, K.A., and Wilk, A. (2007) The Journal of Biological Chemistry **282**, 15126-15136

28. Chan, A. C. K., Lelj-Garolla, B. Rosell, F. I., Pedersen, K. A., Mauk, A. G., and Murphy, M. E. P. (2006) Journal of Molecular Biology **362**, 1108-1119

29. Andreoni, F., Boiani, R., Serafani, G., Bainconi, I., Dominici, S., Gorini, F., and Magnani, M. (2009) Bioscience Biotechnology and Biochemistry **73 (5)**, 1180-1183

30. Tong, Y., and Guo, M. (2009) Archives of Biochemistry and Biophysics **481**, 1-15